Analysis of transfer procedures in elastoplasticity based on the error in the constitutive equations: Theory and numerical illustration

A. Orlando and D. Perić[*,†]

School of Engineering, University of Wales Swansea, Singleton Park, SA2 8PP Swansea, U.K.

SUMMARY

The aim of this work is to illustrate a methodology for the assessment of adaptive strategies for the solution of associative rate-independent plasticity problems solved by employing the incremental displacement conforming finite element method. This is the first step towards a more rational definition of transfer operators in terms of the ensuing error. The motivating idea is the observation that change of data and/or finite element mesh from one time interval to the other can be both related to a discontinuity jump of the approximate solution across the time instant t_n. Thus, reliable *a posteriori* estimates will have to depend not only on the time step and finite element mesh size but also on the value of the jump. A new error estimate based on the error in the constitutive equations is developed which allows characterization of the discontinuity jump. Copyright © 2004 John Wiley & Sons, Ltd.

KEY WORDS: associative rate-independent plasticity; displacement finite element solution; transfer operators; error in the constitutive equations

1. INTRODUCTION

Use of adaptive strategies in solid mechanics for the finite element solution of history-dependent non-linear problems solved by employing incremental methods is of paramount importance. An adaptive strategy can be defined as a computational procedure which delivers the finite element solution for the problem at hand to the prescribed accuracy. Key ingredients are: (i) the availability of an error estimator which accounts for the sources of error associated with the approximation, (ii) error indicators for the choice of the optimal discretization parameters, and (iii) a data transfer procedure when the current finite element mesh is different from the one of the previous time step.

In the finite element analysis of these problems the quality of the simulation is generally assessed by physical or heuristic arguments based on the experience and judgement of the

---
*Correspondence to: D. Perić, School of Engineering, University of Wales Swansea, Singleton Park, SA2 8PP Swansea, U.K.
†E-mail: d.peric@swansea.ac.uk

analyst. Frequently such arguments are specific for the problem under consideration [1–4] and often fail to account for all the discretizations introduced [5–8].

An *a posteriori* error estimation for the solution of the fully discrete scheme has been given in [9, 10]. In Reference [9] error estimates are obtained from the dual analysis applied to the linearized equation that defines the error, whereas in Reference [10] estimates of time and space discretization error are obtained further to heuristic considerations motivated by the physics of the phenomenon.

A family of error measures with clear physical meaning and capable to account for effects of time and space discretization is given by the error in the constitutive equations. The notion, introduced by Ladevèze in 1975 [11] for linear problems, was then extended to history-dependent materials defined by a functional formalism in Reference [12] and to constitutive models with internal variables and having an associative flow rule in Reference [13]. For the latter class of models, the concept of dissipation error was introduced which is related to the residual in the evolution law produced by time continuous admissible solutions that satisfy the compatibility relations, the equilibrium equations, the state law and the initial conditions. The dissipation error was then extended in Reference [14] by removing the state laws from the admissibility conditions. Applications of this error measure were given for an elastic-damage coupled model in Reference [14] solved with the nonincremental LATIN method and to the Prandtl–Reuss plasticity model in Reference [15] solved with the classical incremental finite element method. In the latter work, in particular, it was shown the capability of the new error measure to account for effects of time and space discretization.

The aim of this work is to describe a methodology for the assessment of adaptive strategies for associative rate-independent plasticity problems solved by employing the incremental displacement conforming finite element method. This is the first step towards a more rational definition of the transfer operator in terms of the ensuing error. The motivating idea is the observation that change of data and/or finite element mesh from one time interval to the other can be both related to a discontinuity jump of the approximate solution across the time instant t_n.

When the finite element mesh is changed at time t_n, two finite element solutions are considered for the same load level: the one at t_n^-, which is associated with the mesh $\mathcal{T}_{h_n}$, (henceforth, called old mesh), and the other at t_n^+, which is associated with the mesh $\mathcal{T}_{h_{n+1}}$, (henceforth, referred to as a new mesh). The solution at t_n^+ is computed by equilibrating the data defined by the specific transfer procedure [16]. Consequently, in general, a discontinuity jump appears in the time linear interpolation of the discrete values across the time node t_n as a result of the change of mesh and transfer procedure.

The residual error, which is obtained by substituting the approximation into the equations that define the initial boundary value problem and representing the forcing in the problem that defines the global error, has two components: One component is regular, which is present also with static finite element mesh and depends essentially on the time step and mesh size. The other component is singular for the presence of the rate quantities $\dot{\varepsilon}^p(\mathbf{x}, t)$, $\dot{\alpha}(\mathbf{x}, t)$ and the discontinuity jump in the time interpolant of ε^p and α. The singular components, therefore, depend on the value of the discontinuities which, for the way the fully discrete schemes are formulated, can be arbitrary. Consequently, in principle, they can have an important influence on the global error.

Since the error depends on the residual, reliable *a posteriori* estimates of the error of such approximations will have to depend not only on the time step and finite element mesh size

but also on the value of the jump, that is, on the singular components of the residual. Such structure of error estimates have been obtained from *a posteriori* error analysis of finite element approximations of parabolic problems [17, 18], degenerate parabolic problems [19] and dynamic problems in solid mechanics [20].

In this work, attention will be given only to the error estimation procedure itself. After this introduction, in Section 2 a simple error analysis of a first order ordinary differential equation, chosen as elementary prototype of the evolution law of the internal variables, shows indeed the influence on the error of the time discontinuity jump. It also appears that only measures of error that account for time discretization effects can reflect the low order regularity of the approximation across the time instant t_n when the change of mesh occurs. As a result, the extended dissipation error introduced in Reference [14] naturally lends itself for this aim. After describing briefly the reference problem in Section 3, the first part of Section 4 recalls the extended dissipation error for time continuous admissible solution whereas in the second part, a new measure of the error in the constitutive equations which accounts for the time discontinuity jump in the admissible solution is defined in Section 4. The theory is developed for rate-independent plasticity material models and leads to the definition of an additional nonnegative term in the extended dissipation error which depends on the jump, in agreement with the error analysis of Section 2. This term and the behaviour of the error component in the state law characterize completely the discontinuity jump. This result motivates the use of the augmented extended dissipation error as basis of a methodology for the assessment of the global accuracy in time of finite element solutions on evolving meshes. Applications of the theory are given in Section 5 for the conforming displacement finite element solution of the Prandtl–Reuss plasticity model solved with incremental procedure. After a critical review of the transfer procedures, criteria to build admissible solutions that are as close as possible to the computed finite element solution are proposed. The applicability of the methodology is finally illustrated in Section 6 on a one dimensional model problem where a detailed study of the transfer operators introduced in References [3, 21, 22] is carried out, with the numerical experiments providing confirmation of the theoretical developments.

2. MOTIVATION: THE ERROR ANALYSIS OF A NON-DIFFERENTIABLE APPROXIMATE SOLUTION OF A 1st ORDER ODE

Consider the scalar initial value problem,

$$\left| \begin{array}{l} \dot{u}(t) + a(t)u(t) = f(t) \quad t \in [0, T] \\ u(0) = u_0 \end{array} \right. \tag{1}$$

with $a(t) \geqslant 0$. The solution of (1) is given by [18]

$$u(t) = \exp[-A(t)]u_0 + \int_0^t \exp[-(A(t) - A(\tau))]f(\tau)\,d\tau \tag{2}$$

where $A(t) = \int_0^t a(\tau)\,d\tau$, so that the following *a priori* estimate is obtained:

$$|u(t)| \leqslant |u_0| + \int_0^t |f(\tau)|\,d\tau \tag{3}$$

for the non-decreasing character of $A = A(t)$ and for being $A(t) \geqslant 0$.

Let $0 = t_1 < \cdots < t_n < \cdots < t_{N+1} = T$ be a partition of the time interval $[0, T]$ of interest and consider a function $U = U(t)$ to be approximation of the problem (1), which is differentiable over the intervals $[t_n, t_{n+1}]$. The function $U = U(t)$ may have jump discontinuities at the time instants t_n, thus we let $U(t_n^+) - U(t_n^-) = \Delta_n$. For $n = 1$, we assume $U(t_1^-) = u_0$, thus $\Delta_1 = U_0 - u_0$. This means that $U = U(t)$ is solution of the following problem:

$$\left|\begin{array}{l} \text{For } n = 1, \ldots, N \\[4pt] \dot{U}(t) + a(t)U(t) = f(t) - R(t) \quad t \in [t_n, t_{n+1}] \\[4pt] U(t_n^+) = U(t_n^-) + \Delta_n \end{array}\right.$$

where $R = R(t)$ is the residual produced by $U = U(t)$ within each time interval $[t_n, t_{n+1}]$ where $U = U(t)$ is differentiable.

The error $e(t) = u(t) - U(t)$ associated with the approximation $U = U(t)$ is, therefore, solution of the following problem:

$$\left|\begin{array}{l} \text{For } n = 1, \ldots, N \\[4pt] \dot{e}(t) + a(t)e(t) = R(t) \quad t \in [t_n, t_{n+1}] \\[4pt] e(t_n) = \Delta_n \end{array}\right. \tag{4}$$

Using for each subinterval $[t_n, t_{n+1}]$ the result given in (2), we obtain

$$e(t) = \sum_{n=1}^{N} \exp[-A(t - t_n)]\Delta_n \beta_n + \int_0^t \exp[-(A(t) - A(\tau))]R(\tau)\,\mathrm{d}\tau \tag{5}$$

where

$$\beta_n = \begin{cases} 0 & \text{if } t \leqslant t_n \\ 1 & \text{if } t > t_n \end{cases}$$

The first term on the r.h.s. of Equation (5) gives the propagation at $t\,(\geqslant t_n)$ of the discontinuity jump Δ_n in the approximate solution $U = U(t)$, whereas the integral term can be interpreted as the sum of the time-elemental contributions to the total error at the time t. The time-elemental contributions are obtained by the propagation at time t of the residual error $R(\tau)\,\mathrm{d}\tau$ produced within the time-elemental interval $[\tau, \tau + \mathrm{d}\tau]$ at time $\tau \leqslant t$.

Remark 2.1
Equation (5) shows the influence of the jump discontinuities on the error. Also, note that for a continuous approximation solution $U = U(t)$, that is, $\Delta_n = 0$, for $n = 1, \ldots, N$, the error depends only on the residual produced within the time intervals where the approximation is differentiable.

Applying (3) and the triangular inequality, we obtain the following *a priori* estimate of the solution (5):

$$|e(t)| \leqslant \sum_{n=1}^{N} |\Delta_n|\beta_n + \int_0^t |R(\tau)|\,\mathrm{d}\tau, \quad \forall t \leqslant T \tag{6}$$

which shows the accumulation in time of the jump discontinuities and of the residual as indication of the pointwise error. From (6), it is immediate to obtain also the following global estimate in time:

$$\sup_{t \leqslant T} |e(t)| \leqslant \sum_{n=1}^{N} |\Delta_n| + \int_0^T |R(\tau)|\, d\tau \tag{7}$$

If $R(t) = 0$, $\forall t \in [t_n, t_{n+1}]$, $\forall n$, that is, the approximate solution $U(t)$ does satisfy exactly equation (1) over each time interval $[t_n, t_{n+1}]$, the second term on the r.h.s. of Equation (5) disappears and the error is due to the occurrence of the jumps in $U = U(t)$ across the time nodes t_n. Finally, this means that the error of the approximate solution $U = U(t)$ is related to the error in the initial data over each time interval.

3. THE IBVP FOR A MODEL WITH INTERNAL VARIABLES

We will assume displacements to be small in the quasi-static evolutive process of the body so that geometry changes and inertial effects may be neglected.

3.1. Equilibrium equation

Denote with $\mathscr{S}$ the linear space of the symmetric second order stress tensors. The statically admissible stress fields, $\boldsymbol{\sigma} = \boldsymbol{\sigma}(\mathbf{x}, t) \in \mathscr{S}$, are such that the weak form of the equilibrium, given by the virtual work, is satisfied, that is

$$\underbrace{\int_\Omega \boldsymbol{\sigma}(\mathbf{x}, t) : \nabla \boldsymbol{\eta}(\mathbf{x})\, d\Omega}_{\langle \boldsymbol{\sigma}, \nabla \boldsymbol{\eta} \rangle} = \underbrace{\int_\Omega \mathbf{b}(\mathbf{x}, t) \cdot \boldsymbol{\eta}(\mathbf{x})\, d\Omega}_{\langle \mathbf{b}, \boldsymbol{\eta} \rangle} + \underbrace{\int_{\partial\Omega_t} \mathbf{t}(\mathbf{x}, t) \cdot \boldsymbol{\eta}(\mathbf{x})\, ds}_{\langle \mathbf{t}, \boldsymbol{\eta} \rangle_{\partial\Omega_t}} \quad \begin{array}{l} \forall \boldsymbol{\eta} \in \mathscr{V}_0, \\[2mm] \forall t \in \mathscr{I} = [0, T] \end{array} \tag{8}$$

where $\mathbf{b} = \mathbf{b}(\mathbf{x}, t)$ and $\mathbf{t} = \mathbf{t}(\mathbf{x}, t)$ are, respectively, the body force and surface traction fields and $\mathscr{V}_0$ is the linear space of the virtual displacements which vanish on $\partial\Omega_d$, whereas $\mathscr{I}$ is the time interval of interest [23].

3.2. Compatibility equations

A displacement field $\mathbf{u} = \mathbf{u}(\mathbf{x}, t)$ is kinematically admissible if it is time continuous, at least once differentiable in space and meets the boundary conditions on $\partial\Omega_d$. We refer to $\mathscr{V}$ as the space of the kinematically admissible displacements.

Let $\mathscr{E}$ be the linear space of the symmetric second order strain tensors. The kinematically admissible strain fields, $\boldsymbol{\varepsilon} = \boldsymbol{\varepsilon}(\mathbf{x}, t) \in \mathscr{E}$, are continuous fields which are obtained from the kinematically admissible displacement fields $\mathbf{u} = \mathbf{u}(\mathbf{x}, t) \in \mathscr{V}$ as follows

$$\boldsymbol{\varepsilon} = \tfrac{1}{2}(\nabla \mathbf{u} + \nabla \mathbf{u}^{\mathrm{T}}) \overset{\text{def}}{=} \nabla_s \mathbf{u} \tag{9}$$

3.3. Constitutive equations

We will focus on constitutive models of rate independent plasticity in isothermal conditions belonging to the class of the so-called standard generalised materials as introduced in Reference

[24]. By exploiting the convex structure of these models, emphasis will be placed especially on scalar equivalent formulations of the tensorial constitutive equations.

A thermodynamically consistent model is obtained by specifying the state variables along with the functional form of the free Helmholtz energy and the complementary laws which describe the time evolution of the internal variables in respect of the Clausius-Duhem inequality. For isothermal processes, the aforementioned inequality is given by

$$-\dot{\psi} + \boldsymbol{\sigma} : \dot{\boldsymbol{\varepsilon}} \geqslant 0 \tag{10}$$

where ψ is the free Helmholtz energy per unit volume defined in terms of the state variables which describe the model, and $\boldsymbol{\sigma} : \dot{\boldsymbol{\varepsilon}}$ is the total external power.

3.3.1. State variables. We assume (i) temperature to be constant with time and uniform in space so that it will not be considered hereafter; (ii) that the total strain can be uniquely decomposed additively into its elastic and plastic part, that is,

$$\boldsymbol{\varepsilon} = \boldsymbol{\varepsilon}^{\mathrm{e}} + \boldsymbol{\varepsilon}^{\mathrm{p}} \tag{11}$$

and finally (iii) that the local state of the material is described by means of additional internal variables $\boldsymbol{\alpha}$ which characterize the internal changes of the material.

3.3.2. Equations of state. The free Helmholtz energy ψ is taken as a sum of two proper strictly convex and lower semicontinuous functions [25, 26] of each of its arguments: $\psi_{\mathrm{e}}(\boldsymbol{\varepsilon}^{\mathrm{e}})$ which is the stored energy due to elastic strain and $\psi_{\mathrm{p}}(\boldsymbol{\alpha})$ which is the stored energy due to plastic and internal parameters related to hardening effects [27]

$$\psi(\boldsymbol{\varepsilon}^{\mathrm{e}}, \boldsymbol{\alpha}) = \psi_{\mathrm{e}}(\boldsymbol{\varepsilon}^{\mathrm{e}}) + \psi_{\mathrm{p}}(\boldsymbol{\alpha})$$

By expanding the Clausius-Duhem inequality which is required to hold for any admissible thermodynamic process $(\boldsymbol{\varepsilon}, \boldsymbol{\varepsilon}^{\mathrm{p}}, \boldsymbol{\alpha})$ [28], we obtain the state equations

$$\boldsymbol{\sigma} = \frac{\partial \psi_{\mathrm{e}}}{\partial \boldsymbol{\varepsilon}^{\mathrm{e}}}(\boldsymbol{\varepsilon}^{\mathrm{e}}) \quad \text{and} \quad \mathbf{A} = \frac{\partial \psi_{\mathrm{p}}}{\partial \boldsymbol{\alpha}}(\boldsymbol{\alpha}) \tag{12}$$

and the associated intrinsic mechanical dissipation

$$\boldsymbol{\sigma} : \dot{\boldsymbol{\varepsilon}}^{\mathrm{p}} - \mathbf{A} : \dot{\boldsymbol{\alpha}} \geqslant 0 \tag{13}$$

where the force-type variable $\mathbf{A}$, defined by the hardening law $(12)_2$ is termed the thermodynamic force conjugate to $\boldsymbol{\alpha}$ [27].

For our subsequent developments, it is useful to consider the following equivalent formulation of the state equations (12) [29, 30]

$$
\begin{aligned}
{}_{\mathrm{e}}^{\mathrm{sl}}\eta_{\mathbf{x},t}^2(\boldsymbol{\sigma}; \boldsymbol{\varepsilon}^{\mathrm{e}}) &\overset{\mathrm{def}}{=} \psi_{\mathrm{e}}(\boldsymbol{\varepsilon}^{\mathrm{e}}) + \psi_{\mathrm{e}}^*(\boldsymbol{\sigma}) - \boldsymbol{\sigma} : \boldsymbol{\varepsilon}^{\mathrm{e}} = 0 \Leftrightarrow \boldsymbol{\sigma} - \frac{\partial \psi_{\mathrm{e}}}{\partial \boldsymbol{\varepsilon}^{\mathrm{e}}}(\boldsymbol{\varepsilon}^{\mathrm{e}}) = \mathbf{0} \\
{}_{\mathrm{p}}^{\mathrm{sl}}\eta_{\mathbf{x},t}^2(\mathbf{A}; \boldsymbol{\alpha}) &\overset{\mathrm{def}}{=} \psi_{\mathrm{p}}(\boldsymbol{\alpha}) + \psi_{\mathrm{p}}^*(\mathbf{A}) - \mathbf{A} : \boldsymbol{\alpha} = 0 \Leftrightarrow \mathbf{A} - \frac{\partial \psi_{\mathrm{p}}}{\partial \boldsymbol{\alpha}}(\boldsymbol{\alpha}) = \mathbf{0}
\end{aligned}
\tag{14}
$$

where $\psi_e^*(\boldsymbol{\sigma})$ and $\psi_p^*(\mathbf{A})$ are the conjugate functions or Legendre–Fenchel transforms [25, 26] of $\psi_e(\boldsymbol{\varepsilon}^e)$ and $\psi_p(\boldsymbol{\alpha})$, respectively. These are defined as

$$\psi_e^* : \boldsymbol{\sigma} \in \mathscr{S} \to \psi_e^*(\boldsymbol{\sigma}) = \sup_{\boldsymbol{\varepsilon}^e \in \mathscr{E}} \{\boldsymbol{\sigma} : \boldsymbol{\varepsilon}^e - \psi_e(\boldsymbol{\varepsilon}^e)\} \in \mathbb{R} \cup \{+\infty\}$$

$$\psi_p^* : \mathbf{A} \in \mathscr{A} \to \psi_p^*(\mathbf{A}) = \sup_{\boldsymbol{\alpha} \in \Lambda} \{\mathbf{A} : \boldsymbol{\alpha} - \psi_p(\boldsymbol{\alpha})\} \in \mathbb{R} \cup \{+\infty\}$$

(15)

with $\boldsymbol{\sigma} : \boldsymbol{\varepsilon}$ denoting the duality pairing of the two spaces $\mathscr{S}$ and $\mathscr{E}$, whereas $\mathbf{A} : \boldsymbol{\alpha}$ is the duality pairing of the space Λ of the strain-type internal variables $\boldsymbol{\alpha}$ and the space $\mathscr{A}$ of the thermodynamic forces $\mathbf{A}$.

Upon the definition of the Legendre–Frenchel transforms, it follows that for any pair $(\boldsymbol{\sigma}, \boldsymbol{\varepsilon}^e) \in \Sigma = \mathscr{S} \times \mathscr{E}$ and $(\boldsymbol{\alpha}, \mathbf{A}) \in \Lambda \times \mathscr{A}$,

$$\psi_e^*(\boldsymbol{\sigma}) + \psi_e(\boldsymbol{\varepsilon}^e) - \boldsymbol{\sigma} : \boldsymbol{\varepsilon}^e \geqslant 0$$

$$\psi_p^*(\mathbf{A}) + \psi_p(\boldsymbol{\alpha}) - \mathbf{A} : \boldsymbol{\alpha} \geqslant 0$$

(16)

where the respective equality applies if and only if $(\boldsymbol{\sigma}, \boldsymbol{\varepsilon}^e)$ is the solution of $(12)_1$ and $(\mathbf{A}, \boldsymbol{\alpha})$ is the solution of $(12)_2$, respectively.

3.3.3. Complementary equations. Associative plasticity. The complementary or evolution laws characterize the history of the observable variables in terms of the internal variables and they are restricted to meet the intrinsic mechanical inequality (13) [31]. A simple way to ensure *a priori* the thermodynamic consistency of the model is given by the class of the standard generalised materials. In these models, one assumes the existence of a potential of dissipation $\varphi(\dot{\boldsymbol{\varepsilon}}^p, -\dot{\boldsymbol{\alpha}})$ in the space $\dot{\Sigma} = \dot{\mathscr{E}} \times \dot{\Lambda}$ of rate of dissipative variables, which is positive, convex in its variables, lower semicontinuous and such that $\varphi(\mathbf{0}, \mathbf{0}) = 0$. The complementary laws are then given by

$$(\boldsymbol{\sigma}, \mathbf{A}) \in \partial \varphi(\dot{\boldsymbol{\varepsilon}}^p, -\dot{\boldsymbol{\alpha}})$$

(17)

where the symbol ∂ denotes the subdifferential operator [25, 26].

For the rate-independent plasticity models, hereafter considered, the dissipation potential $\varphi(\dot{\boldsymbol{\varepsilon}}^p, -\dot{\boldsymbol{\alpha}})$ may be characterized as the support function of a closed convex domain $\mathbb{E} \subseteq \Sigma$, containing the origin $(\boldsymbol{\sigma}, \mathbf{A}) = (\mathbf{0}, \mathbf{0})$, that is,

$$\varphi(\dot{\boldsymbol{\varepsilon}}^p, -\dot{\boldsymbol{\alpha}}) = \sup_{(\boldsymbol{\sigma}, \mathbf{A}) \in \mathbb{E}} \{\boldsymbol{\sigma} : \dot{\boldsymbol{\varepsilon}}^p - \mathbf{A} : \dot{\boldsymbol{\alpha}}\}, \quad \forall (\dot{\boldsymbol{\varepsilon}}^p, -\dot{\boldsymbol{\alpha}}) \in \dot{\Sigma}$$

(18)

with $\mathbb{E}$, called the elastic domain, defined by

$$\mathbb{E} = \{(\boldsymbol{\sigma}, \mathbf{A}) \in \Sigma \mid \boldsymbol{\sigma} : \dot{\boldsymbol{\varepsilon}}^p - \mathbf{A} : \dot{\boldsymbol{\alpha}} \leqslant \varphi(\dot{\boldsymbol{\varepsilon}}^p, -\dot{\boldsymbol{\alpha}}), \quad \forall (\dot{\boldsymbol{\varepsilon}}^p, -\dot{\boldsymbol{\alpha}}) \in \dot{\Sigma}\}$$

(19)

and representing the locus of the admissible generalized stresses.

In place of Equation (17), it is usually more convenient to refer to the inverse relations obtained by introducing the Legendre–Fenchel transform of φ defined as

$$\varphi^* : (\boldsymbol{\sigma}, \mathbf{A}) \in \mathscr{S} \times \mathscr{A} \to \varphi^*(\boldsymbol{\sigma}, \mathbf{A}) = \sup_{(\dot{\boldsymbol{\varepsilon}}^p, -\dot{\boldsymbol{\alpha}}) \in \dot{\Sigma}} \{\boldsymbol{\sigma} : \dot{\boldsymbol{\varepsilon}}^p - \mathbf{A} : \dot{\boldsymbol{\alpha}} - \varphi(\dot{\boldsymbol{\varepsilon}}^p, -\dot{\boldsymbol{\alpha}})\}$$

Since $\varphi(\dot{\boldsymbol{\varepsilon}}^{\mathrm{p}}, -\dot{\boldsymbol{\alpha}})$ is the support function of $\mathbb{E}$, the dual dissipation potential $\varphi^*(\boldsymbol{\sigma}, \mathbf{A})$ is then the indicator function of $\mathbb{E}$ defined as

$$\varphi^*(\boldsymbol{\sigma}, \mathbf{A}) = I_{\mathbb{E}} \stackrel{\mathrm{def}}{=} \begin{cases} 0 & \text{if } (\boldsymbol{\sigma}, \mathbf{A}) \in \mathbb{E} \\ +\infty & \text{if } (\boldsymbol{\sigma}, \mathbf{A}) \notin \mathbb{E} \end{cases}$$

The evolution equations for the internal variables can therefore be expressed also as

$$(\dot{\boldsymbol{\varepsilon}}^{\mathrm{p}}, -\dot{\boldsymbol{\alpha}}) \in \partial\varphi^*(\boldsymbol{\sigma}, \mathbf{A}) \tag{20}$$

For our subsequent developments, likewise for the state equations, the evolution laws are recast into an equivalent formulation [23, 29] which exploits the convexity of the model,

$$^{d}\eta_{\mathbf{x},t}^2(\boldsymbol{\sigma}, \mathbf{A}; \dot{\boldsymbol{\varepsilon}}^{\mathrm{p}}, \dot{\boldsymbol{\alpha}}) \stackrel{\mathrm{def}}{=} \varphi(\dot{\boldsymbol{\varepsilon}}^{\mathrm{p}}, -\dot{\boldsymbol{\alpha}}) + \varphi^*(\boldsymbol{\sigma}, \mathbf{A}) - \boldsymbol{\sigma} : \dot{\boldsymbol{\varepsilon}}^{\mathrm{p}}$$

$$+ \mathbf{A} : \dot{\boldsymbol{\alpha}} = 0 \Leftrightarrow (\dot{\boldsymbol{\varepsilon}}^{\mathrm{p}}, -\dot{\boldsymbol{\alpha}}) \in \partial\varphi^*(\boldsymbol{\sigma}, \mathbf{A}) \tag{21}$$

From the properties of the Legendre–Fenchel transform, it follows that for any state $(\boldsymbol{\sigma}, \mathbf{A}; \dot{\boldsymbol{\varepsilon}}^{\mathrm{p}}, -\dot{\boldsymbol{\alpha}}) \in \Sigma \times \dot{\Sigma}$

$$\varphi(\dot{\boldsymbol{\varepsilon}}^{\mathrm{p}}, -\dot{\boldsymbol{\alpha}}) + \varphi^*(\boldsymbol{\sigma}, \mathbf{A}) - \boldsymbol{\sigma} : \dot{\boldsymbol{\varepsilon}}^{\mathrm{p}} + \mathbf{A} : \dot{\boldsymbol{\alpha}} \geqslant 0 \tag{22}$$

where the equality holds if and only if $(\boldsymbol{\sigma}, \mathbf{A}; \dot{\boldsymbol{\varepsilon}}^{\mathrm{p}}, \dot{\boldsymbol{\alpha}})$ is a solution of (20).

Finally, for the quasi-static process where inertial effects are neglected, the initial conditions for the variables appearing in rate form have to be given to complete the initial boundary value problem. These are given by

$$\boldsymbol{\varepsilon}^{\mathrm{p}}(\mathbf{x}, t = 0) = \boldsymbol{\varepsilon}_0^{\mathrm{p}}(\mathbf{x}) \quad \text{and} \quad \boldsymbol{\alpha}(\mathbf{x}, t = 0) = \boldsymbol{\alpha}_0(\mathbf{x})$$

The initial boundary value problem for this class of models is summarized in Box 1.

3.4. The Prandtl–Reuss plasticity model

The Prandtl–Reuss plasticity model is a standard model obtained by using the Von Mises yield criterion and an isotropic hardening law. The internal variables are the plastic strain tensor $\boldsymbol{\varepsilon}^{\mathrm{p}}$ and the accumulated plastic strain p, while the conjugate variables are the stress tensor $\boldsymbol{\sigma}$ and the thermodynamic force R, respectively.

3.4.1. State laws. The free Helmholtz energy is chosen as

$$\psi(\boldsymbol{\varepsilon}^{\mathrm{e}}, p) = \psi_{\mathrm{e}}(\boldsymbol{\varepsilon}^{\mathrm{e}}) + \psi_{\mathrm{p}}(p) = \frac{1}{2}\mathbf{C}\boldsymbol{\varepsilon}^{\mathrm{e}} : \boldsymbol{\varepsilon}^{\mathrm{e}} + \int_0^p g(q)\,\mathrm{d}q$$

with $\mathbf{C}$ being the Hooke elasticity tensor and $g(p)$ is a positive and increasing scalar function of the accumulated plastic strain p with $g(p = 0) = 0$. Also, it results

$$\psi^*(\boldsymbol{\sigma}, R) = \psi_{\mathrm{e}}^*(\boldsymbol{\sigma}) + \psi_{\mathrm{p}}^*(R) = \frac{1}{2}\mathbf{C}^{-1}\boldsymbol{\sigma} : \boldsymbol{\sigma} + Rg^{-1}(R) - \psi_{\mathrm{p}}(g^{-1}(R))$$

<div style="text-align: center;">Box 1. IBVP for standard generalized models with internal variables.</div>

Data $\mathbf{b}(\mathbf{x}, t)$ on Ω, $\mathbf{t}(\mathbf{x}, t)$ on $\partial\Omega_t$ and $\mathbf{u}_0(\mathbf{x}, t)$ on $\partial\Omega_d$
Find $\boldsymbol{\sigma}(\mathbf{x}, t), \mathbf{A}(\mathbf{x}, t)$; $\mathbf{u}(\mathbf{x}, t), \boldsymbol{\varepsilon}(\mathbf{x}, t), \boldsymbol{\varepsilon}^{\mathrm{p}}(\mathbf{x}, t), \boldsymbol{\alpha}(\mathbf{x}, t)$ such that the following conditions are satisfied:

(a)
Kinematic Compatibility:
Continuity of the Displacement Field, $\mathbf{u}(\mathbf{x}, t)$.
Time continuity of the Total Strain, $\boldsymbol{\varepsilon}(\mathbf{x}, t) = \nabla_s \mathbf{u}(\mathbf{x}, t)$.
Time continuity of the Plastic Strain, $\boldsymbol{\varepsilon}^{\mathrm{p}}(\mathbf{x}, t)$.
Time continuity of the Internal Variables, $\boldsymbol{\alpha}(\mathbf{x}, t)$.
Displacement Boundary Conditions.

(b)
Equilibrium:
$$\langle \boldsymbol{\sigma}(\mathbf{x}, t), \; \nabla\boldsymbol{\eta}(\mathbf{x})\rangle = \langle \mathbf{b}(\mathbf{x}, t), \boldsymbol{\eta}(\mathbf{x})\rangle + \langle \mathbf{t}(\mathbf{x}, t), \boldsymbol{\eta}(\mathbf{x})\rangle_{\partial\Omega_t}$$
$$\forall \boldsymbol{\eta} \in \mathscr{V}_0, \quad \forall t \in [0, T].$$

<div style="text-align: center;">**The constitutive initial value problem**</div>

(c)
Additivity of the Strain Tensor:
$$\boldsymbol{\varepsilon}(\mathbf{x}, t) = \boldsymbol{\varepsilon}^{\mathrm{e}}(\mathbf{x}, t) + \boldsymbol{\varepsilon}^{\mathrm{p}}(\mathbf{x}, t),$$
$$\forall \mathbf{x} \in \Omega, \; \forall t \in [0, T].$$

(d)
State Laws:
$$\psi_{\mathrm{e}}(\boldsymbol{\varepsilon}^{\mathrm{e}}(\mathbf{x}, t)) + \psi_{\mathrm{e}}^*(\boldsymbol{\sigma}(\mathbf{x}, t)) - \boldsymbol{\sigma}(\mathbf{x}, t) : \boldsymbol{\varepsilon}^{\mathrm{e}}(\mathbf{x}, t) = 0 \Leftrightarrow \boldsymbol{\sigma} - \frac{\partial\psi_{\mathrm{e}}}{\partial\boldsymbol{\varepsilon}^{\mathrm{e}}}(\boldsymbol{\varepsilon}^{\mathrm{e}}) = 0,$$
$$\psi_{\mathrm{p}}(\boldsymbol{\alpha}(\mathbf{x}, t)) + \psi_{\mathrm{p}}^*(\mathbf{A}(\mathbf{x}, t)) - \mathbf{A}(\mathbf{x}, t) : \boldsymbol{\alpha}(\mathbf{x}, t) = 0 \Leftrightarrow \mathbf{A} - \frac{\partial\psi_{\mathrm{p}}}{\partial\boldsymbol{\alpha}}(\boldsymbol{\alpha}) = 0,$$
$$\forall \mathbf{x} \in \Omega, \; \forall t \in [0, T].$$

(e)
Evolution Laws:
$$\varphi(\dot{\boldsymbol{\varepsilon}}^{\mathrm{p}}(\mathbf{x}, t), -\dot{\boldsymbol{\alpha}}(\mathbf{x}, t)) + \varphi^*(\boldsymbol{\sigma}(\mathbf{x}, t), \mathbf{A}(\mathbf{x}, t))$$
$$-\boldsymbol{\sigma}(\mathbf{x}, t) : \dot{\boldsymbol{\varepsilon}}^{\mathrm{p}}(\mathbf{x}, t) + \mathbf{A}(\mathbf{x}, t) : \dot{\boldsymbol{\alpha}}(\mathbf{x}, t) = 0 \Leftrightarrow (\dot{\boldsymbol{\varepsilon}}^{\mathrm{p}}, -\dot{\boldsymbol{\alpha}}) \in \partial\varphi^*(\boldsymbol{\sigma}, \mathbf{A}),$$
$$\forall \mathbf{x} \in \Omega, \; \forall t \in [0, T].$$

(f)
Initial Conditions:
$$\boldsymbol{\varepsilon}^{\mathrm{p}}(\mathbf{x}, t = 0) = \mathbf{0},$$
$$\boldsymbol{\alpha}(\mathbf{x}, t = 0) = \mathbf{0}, \qquad \forall \mathbf{x} \in \Omega$$

therefore, the state laws can be formulated as follows

$$\psi_{\mathrm{e}}(\boldsymbol{\varepsilon}^{\mathrm{e}}) + \psi_{\mathrm{e}}^*(\boldsymbol{\sigma}) - \boldsymbol{\sigma} : \boldsymbol{\varepsilon}^{\mathrm{e}} = 0 \quad \text{and} \quad \psi_{\mathrm{p}}(p) + \psi_{\mathrm{p}}^*(R) - Rp = 0$$

where ψ_{e}^* and ψ_{p}^* denote the Legendre transforms of ψ_{e} and ψ_{p}, respectively.

3.4.2. Evolution laws. Given the closed convex elastic domain,

$$\mathbb{E} = \{(\boldsymbol{\sigma}, R) \mid \|\boldsymbol{\sigma}_D\| - (R + R_0) \leqslant 0, \quad R \geqslant 0\}$$

with R_0 the initial yield stress, the dissipation potential is [23]

$$\varphi(\dot{\boldsymbol{\varepsilon}}^{\mathrm{p}}, -\dot{p}) = \sup_{(\boldsymbol{\sigma}, R) \in \mathbb{E}} \{\boldsymbol{\sigma} : \dot{\boldsymbol{\varepsilon}}^{\mathrm{p}} - R\dot{p}\} = R_0 \|\dot{\boldsymbol{\varepsilon}}^{\mathrm{p}}\| + I_{\mathbb{C}}$$

with $I_{\mathbb{C}}$ being the indicator function of the following closed convex set:

$$\mathbb{C} = \{(\dot{\boldsymbol{\varepsilon}}^{\mathrm{p}}, -\dot{p}) \mid \|\dot{\boldsymbol{\varepsilon}}^{\mathrm{p}}\| - \dot{p} \leqslant 0 \quad \text{and} \quad \mathrm{Tr}[\dot{\boldsymbol{\varepsilon}}^{\mathrm{p}}] = 0\}$$

The dual dissipation potential $\varphi^*(\boldsymbol{\sigma}, R)$ is the indicator function of $\mathbb{E}$, i.e.

$$\varphi^*(\boldsymbol{\sigma}, R) = I_{\mathbb{E}}$$

The evolution laws can, therefore, be formulated as follows:

$$\varphi^*(\boldsymbol{\sigma}, R) + \varphi(\dot{\boldsymbol{\varepsilon}}^{\mathrm{p}}, -\dot{p}) - \boldsymbol{\sigma} : \dot{\boldsymbol{\varepsilon}}^{\mathrm{p}} + R\dot{p} = 0$$

4. ADMISSIBLE SOLUTION AND MEASURE OF THE ERROR

We assume that the problem of computing the response of the model described in the previous section and summarized in Box 1 is posed by the set of functions, $(\boldsymbol{\sigma}(\mathbf{x}, t), \mathbf{A}(\mathbf{x}, t); \boldsymbol{\varepsilon}(\mathbf{x}, t), \boldsymbol{\varepsilon}^{\mathrm{p}}(\mathbf{x}, t), \boldsymbol{\alpha}(\mathbf{x}, t))$, which gives a finite value to the global energy

$$\int_{\Omega} {}^{\mathrm{sl}}_{\mathrm{e}} \eta^2_{\mathbf{x}, t}(\boldsymbol{\sigma}; \boldsymbol{\varepsilon}^{\mathrm{e}}) \, \mathrm{d}\Omega + \int_{\Omega} {}^{\mathrm{sl}}_{\mathrm{p}} \eta^2_{\mathbf{x}, t}(\mathbf{A}; \boldsymbol{\alpha}) \, \mathrm{d}\Omega + \int_{\Omega} \int_0^T {}^{\mathrm{d}} \eta^2_{\mathbf{x}, t}(\boldsymbol{\sigma}, \mathbf{A}; \dot{\boldsymbol{\varepsilon}}^{\mathrm{p}}, \dot{\boldsymbol{\alpha}}) \, \mathrm{d}t \, \mathrm{d}\Omega < \infty$$

Also, we assume that the formulation is such that the problem has a solution which is unique.

In this class of functions, we distinguish a subset given by those functions which satisfy *only some* properties and equations given in Box 1. Any element of this set is referred to, in general, as an *admissible solution*. It is, therefore, clear that an admissible solution is the exact solution if and only if also *the remaining* equations are satisfied. Given the dissipative character of the problem under consideration, a direct measure of the residual related to these remaining equations can be used as an indication of the error associated with the problem [32].

4.1. The extended dissipation error

The extended dissipation error introduced in Reference [14] is an error in the formulation with internal variables of the constitutive equations. Only the compatibility and equilibrium equations are assumed for the definition of the admissibility conditions. More precisely, the field $(\boldsymbol{\sigma}_{\mathrm{ad}}(\mathbf{x}, t), \mathbf{A}_{\mathrm{ad}}(\mathbf{x}, t); \mathbf{u}_{\mathrm{ad}}(\mathbf{x}, t), \boldsymbol{\varepsilon}_{\mathrm{ad}}(\mathbf{x}, t), \boldsymbol{\varepsilon}^{\mathrm{p}}_{\mathrm{ad}}(\mathbf{x}, t), \boldsymbol{\alpha}_{\mathrm{ad}}(\mathbf{x}, t))$ is an admissible solution with respect to the computation of the extended dissipation error if conditions (a), (b), (c) and (f) given in Box 1 are met.

4.1.1. Definition of error. The equations that are not satisfied by the above admissible solution are the state laws and the evolution laws. Therefore, the quality of the admissible solution depends upon the residual produced therein. A natural way to measure this residual is obtained by resorting to the equivalent scalar formulations of the state and evolution laws given by (14) and (21), respectively. Furthermore, given the nature of the state laws that relate the current value of the kinematic variables to the corresponding static one, a global measure of the error is obtained by assuming an L^∞ accumulation in time of the current value of the error in the state laws. Therefore, it is quite natural to assume the following definition of error:

$$
e_{\mathrm{ext}}^2(T) = \sup_{t \leqslant T} \left\{ \overbrace{\underbrace{2 \int_\Omega {}^{\mathrm{sl}}\eta_{\mathbf{x},t}^2(\boldsymbol{\sigma}_{\mathrm{ad}}, \mathbf{A}_{\mathrm{ad}};\ \boldsymbol{\varepsilon}_{\mathrm{ad}}^{\mathrm{e}}, \boldsymbol{\alpha}_{\mathrm{ad}})\, \mathrm{d}\Omega}_{\theta_{\mathrm{sl}}^2(t)} + \underbrace{2 \int_\Omega \int_0^t {}^{\mathrm{d}}\eta_{\mathbf{x},\tau}^2(\boldsymbol{\sigma}_{\mathrm{ad}}, \mathbf{A}_{\mathrm{ad}};\ \dot{\boldsymbol{\varepsilon}}_{\mathrm{ad}}^{\mathrm{p}}, \dot{\boldsymbol{\alpha}}_{\mathrm{ad}})\, \mathrm{d}\tau\, \mathrm{d}\Omega}_{\theta_{\mathrm{d}}^2(t)}}^{\theta^2(t)} \right\}
$$

$$(23)$$

where, in general, the quantity

$$
{}^{\mathrm{sl}}\eta_{\mathbf{x},t}^2(\boldsymbol{\sigma}_{\mathrm{ad}}, \mathbf{A}_{\mathrm{ad}};\ \boldsymbol{\varepsilon}_{\mathrm{ad}}^{\mathrm{e}}, \boldsymbol{\alpha}_{\mathrm{ad}}) = \psi^*(\boldsymbol{\sigma}_{\mathrm{ad}}(\mathbf{x}, t), \mathbf{A}_{\mathrm{ad}}(\mathbf{x}, t)) + \psi(\boldsymbol{\varepsilon}_{\mathrm{ad}}^{\mathrm{e}}(\mathbf{x}, t), \boldsymbol{\alpha}_{\mathrm{ad}}(\mathbf{x}, t))
$$

$$
- \boldsymbol{\sigma}_{\mathrm{ad}}(\mathbf{x}, t) : \boldsymbol{\varepsilon}_{\mathrm{ad}}^{\mathrm{e}}(\mathbf{x}, t) - \mathbf{A}_{\mathrm{ad}}(\mathbf{x}, t) : \boldsymbol{\alpha}_{\mathrm{ad}}(\mathbf{x}, t)
$$

is the residual in the state laws and the term

$$
{}^{\mathrm{d}}\eta_{\mathbf{x},t}^2(\boldsymbol{\sigma}_{\mathrm{ad}}, \mathbf{A}_{\mathrm{ad}};\ \dot{\boldsymbol{\varepsilon}}_{\mathrm{ad}}^{\mathrm{p}}, \dot{\boldsymbol{\alpha}}_{\mathrm{ad}}) = \varphi^*(\boldsymbol{\sigma}_{\mathrm{ad}}(\mathbf{x}, t), \mathbf{A}_{\mathrm{ad}}(\mathbf{x}, t)) + \varphi(\dot{\boldsymbol{\varepsilon}}_{\mathrm{ad}}^{\mathrm{p}}(\mathbf{x}, t), -\dot{\boldsymbol{\alpha}}_{\mathrm{ad}}(\mathbf{x}, t))
$$

$$
- \boldsymbol{\sigma}_{\mathrm{ad}}(\mathbf{x}, t) : \dot{\boldsymbol{\varepsilon}}_{\mathrm{ad}}^{\mathrm{p}}(\mathbf{x}, t) + \mathbf{A}_{\mathrm{ad}}(\mathbf{x}, t) : \dot{\boldsymbol{\alpha}}_{\mathrm{ad}}(\mathbf{x}, t)
$$

describes the residual produced in the evolution laws.

If we denote by

$$
s_{\mathrm{ad}}(\mathbf{x}, t) = (\boldsymbol{\sigma}_{\mathrm{ad}}(\mathbf{x}, t), \mathbf{A}_{\mathrm{ad}}(\mathbf{x}, t);\ \boldsymbol{\varepsilon}_{\mathrm{ad}}(\mathbf{x}, t), \boldsymbol{\varepsilon}_{\mathrm{ad}}^{\mathrm{p}}(\mathbf{x}, t), \boldsymbol{\alpha}_{\mathrm{ad}}(\mathbf{x}, t))
$$

and

$$
s_{\mathrm{ex}}(\mathbf{x}, t) = (\boldsymbol{\sigma}_{\mathrm{ex}}(\mathbf{x}, t), \mathbf{A}_{\mathrm{ex}}(\mathbf{x}, t); \boldsymbol{\varepsilon}_{\mathrm{ex}}(\mathbf{x}, t),\ \boldsymbol{\varepsilon}_{\mathrm{ex}}^{\mathrm{p}}(\mathbf{x}, t), \boldsymbol{\alpha}_{\mathrm{ex}}(\mathbf{x}, t))
$$

an admissible and the exact solution of the initial boundary value problem, respectively, Definition (23) can be assumed as a global measure of the error of the (kinematic) admissible solution in the following sense:

Proposition 1
Given an admissible solution $s_{\mathrm{ad}} = s_{\mathrm{ad}}(\mathbf{x}, t)$ with respect to the computation of the extended dissipation error, it follows:

$$
e_{\mathrm{ext}}^2(T) \geqslant 0
$$

$$
e_{\mathrm{ext}}^2(T) = 0 \Longleftrightarrow s_{\mathrm{ad}}(\mathbf{x}, t) = s_{\mathrm{ex}}(\mathbf{x}, t) \quad \forall \mathbf{x} \in \Omega, \quad \forall t \leqslant T
$$

$$(24)$$

Proof
Statement $(24)_1$ follows easily from (16) and (22), whereas $(24)_2$ derives from the non-negativity and non-decreasing nature of $e_{\text{ext}}^2(t)$ and the characterizations (14) and (21).

4.2. The error in the evolution law for admissible solution with jump at t_n

In this section, we want to show how the error component in the evolution law can be extended to the case in which the hypothesis of time continuity is removed so that admissible solutions may include a discontinuity jump at a given time instant t_n, i.e. $s_{\text{ad}}(\mathbf{x}, t_n^-) \neq s_{\text{ad}}(\mathbf{x}, t_n^+)$.

In case of the rate independent plasticity, the solution of the initial boundary value problem which governs the evolution of the continuum depends only on the sequence of load levels whereas time has just the function of ordering this sequence. In agreement with this behaviour, it can be assumed that the value of the admissible solution at t_n^+ is also the value at $t_n + \Delta t$ and is independent on Δt. In this way, a fictitious time continuous process over the time interval $[t_n, t_n + \Delta t]$ along which the discontinuity is assumed to be taking place can be defined, and one can analyse the error in the evolution law as the time step Δt shrinks to zero.

Under constant load level equal to $\mathbf{b}(\mathbf{x}, t_n)$, we consider a fundamental family [33] of fictitious time continuous admissible solutions $(\bullet)_{\text{ad}, \Delta t}(\mathbf{x}, \tau)$ over $[t_n, t_n + \Delta t]$ and parameterized by Δt having as limit the given admissible solution, that is, we consider $\forall \mathbf{x} \in \Omega$,

$$\lim_{\Delta t \to 0+} \boldsymbol{\sigma}_{\text{ad}, \Delta t}(\mathbf{x}, \tau) = \boldsymbol{\sigma}_{\text{ad}}(\mathbf{x}, \tau); \qquad \lim_{\Delta t \to 0+} \mathbf{A}_{\text{ad}, \Delta t}(\mathbf{x}, \tau) = \mathbf{A}_{\text{ad}}(\mathbf{x}, \tau)$$

$$\lim_{\Delta t \to 0+} \boldsymbol{\varepsilon}_{\text{ad}, \Delta t}(\mathbf{x}, \tau) = \boldsymbol{\varepsilon}_{\text{ad}}(\mathbf{x}, \tau); \qquad \lim_{\Delta t \to 0+} \boldsymbol{\varepsilon}^{\text{p}}_{\text{ad}, \Delta t}(\mathbf{x}, \tau) = \boldsymbol{\varepsilon}^{\text{p}}_{\text{ad}}(\mathbf{x}, \tau); \qquad \lim_{\Delta t \to 0+} \boldsymbol{\alpha}_{\text{ad}, \Delta t}(\mathbf{x}, \tau) = \boldsymbol{\alpha}_{\text{ad}}(\mathbf{x}, \tau)$$

where $(\bullet)_{\text{ad}}(\mathbf{x}, \tau)$ denote the functions with the time discontinuity jump.

With regard to each member of this family, the error in the evolution law can now be computed. Thus, if $\forall \mathbf{x} \in \Omega$ the following limit exists and is finite:

$$\Delta \zeta_d^2(\mathbf{x}, t_n) \equiv \lim_{\Delta t \to 0+} \int_{t_n}^{t_n + \Delta t} {}^{d, \Delta t}\eta^2_{\mathbf{x}, \tau}(\boldsymbol{\sigma}_{\text{ad}, \Delta t}, \mathbf{A}_{\text{ad}, \Delta t}; \ \dot{\boldsymbol{\varepsilon}}^{\text{p}}_{\text{ad}, \Delta t}, -\dot{\boldsymbol{\alpha}}_{\text{ad}, \Delta t}) \, \mathrm{d}\tau \qquad (25)$$

where

$$
{}^{d, \Delta t}\eta^2_{\mathbf{x}, \tau} = \varphi^*(\boldsymbol{\sigma}_{\text{ad}, \Delta t}(\mathbf{x}, \tau), \mathbf{A}_{\text{ad}, \Delta t}(\mathbf{x}, \tau)) + \varphi(\dot{\boldsymbol{\varepsilon}}^{\text{p}}_{\text{ad}, \Delta t}(\mathbf{x}, \tau), -\dot{\boldsymbol{\alpha}}_{\text{ad}, \Delta t}(\mathbf{x}, \tau))
$$

$$
- \boldsymbol{\sigma}_{\text{ad}, \Delta t}(\mathbf{x}, \tau) : \dot{\boldsymbol{\varepsilon}}^{\text{p}}_{\text{ad}, \Delta t}(\mathbf{x}, \tau) + \mathbf{A}_{\text{ad}, \Delta t}(\mathbf{x}, \tau) : \dot{\boldsymbol{\alpha}}_{\text{ad}, \Delta t}(\mathbf{x}, \tau)
$$

it seems natural to assume the limit to be the error in the evolution law at the point $\mathbf{x}$ in presence of discontinuity.

Remark 4.1
In order to have a finite value for the error, the fictitious time continuous admissible solutions are required to belong to the effective domain of the functional ${}^{d, \Delta t}\eta^2_{\mathbf{x}, \tau}$. Furthermore, the additional term, ${}^{\Delta}\zeta_d^2(\mathbf{x}, t_n)$, is always non-negative as a result of the limit of non-negative functions due to the Legendre–Fenchel inequality. Thus, the jump in the admissible solution

will always produce a non-negative contribution to the error component associated with the dissipation.

4.2.1. Augmented extended dissipation error. The error in the constitutive equations at the time T of the admissible solution with jump across the time $t_n \in]0, T[$ is given by [32]

$$
\Delta e_{\text{ext}}^2(T) = \sup_{t \leqslant T} \left\{ \underbrace{2 \int_\Omega {}^{\text{sl}}\eta_{\mathbf{x},t}^2(\boldsymbol{\sigma}_{\text{ad}}, \mathbf{A}_{\text{ad}}; \boldsymbol{\varepsilon}_{\text{ad}}^{\text{e}}, \boldsymbol{\alpha}_{\text{ad}}) \, \mathrm{d}\Omega}_{\theta_{\text{sl}}^2(t)} \right.
$$

$$
\left. + \underbrace{2 \int_\Omega \int_0^t {}^d\eta_{\mathbf{x},\tau}^2(\boldsymbol{\sigma}_{\text{ad}}, \mathbf{A}_{\text{ad}}; \dot{\boldsymbol{\varepsilon}}_{\text{ad}}^{\text{p}}, \dot{\boldsymbol{\alpha}}_{\text{ad}}) \, \mathrm{d}\tau \, \mathrm{d}\Omega + 2 \int_\Omega {}^\Delta\zeta_d^2(\mathbf{x}, t_n) \, \mathrm{d}\Omega}_{\theta_d^2(t)} \right\} \tag{26}
$$

where ${}^\Delta\zeta_d^2(\mathbf{x}, t_n)$ is defined by (25).

Remark 4.2
Starting from a different point of view, the additional term due to the discontinuity jump appears also in the error analysis carried out in Reference [9]. The authors refer to a dual variational formulation of plasticity and propose a splitting of the error which distinguishes the component due (i) to time discretization, (ii) to the space discretization and (iii) to the effect, through the stability of the non-linear incremental boundary value problem, of the error for using different data in posing this problem.

For the Prandtl–Reuss plasticity model, ${}^\Delta\zeta_d^2(\mathbf{x}, t_n)$ is given by

$$
{}^\Delta\zeta_d^2(\mathbf{x}, t_n) = R_0 \|\boldsymbol{\varepsilon}_{\text{ad}}^{\text{p}}(\mathbf{x}, t_n^+) - \boldsymbol{\varepsilon}_{\text{ad}}^{\text{p}}(\mathbf{x}, t_n^-)\| - \frac{\boldsymbol{\sigma}_{\text{ad}}(\mathbf{x}, t_n^+) + \boldsymbol{\sigma}_{\text{ad}}(\mathbf{x}, t_n^-)}{2} : (\boldsymbol{\varepsilon}_{\text{ad}}^{\text{p}}(\mathbf{x}, t_n^+) - \boldsymbol{\varepsilon}_{\text{ad}}^{\text{p}}(\mathbf{x}, t_n^-))
$$

$$
+ \frac{R_{\text{ad}}(\mathbf{x}, t_n^+) + R_{\text{ad}}(\mathbf{x}, t_n^-)}{2} (p_{\text{ad}}(\mathbf{x}, t_n^+) - p_{\text{ad}}(\mathbf{x}, t_n^-)), \quad \forall \mathbf{x} \in \Omega \tag{27}
$$

The expression of ${}^\Delta\zeta_d^2(\mathbf{x}, t_n)$ is obtained by assuming fictitious continuous admissible solutions $(\bullet)_{\text{ad},\Delta t}(\mathbf{x}, \tau)$ as linear interpolations of the values at t_n^- and t_n^+ over $[t_n, t_n + \Delta t]$ and computing the limit (25) [32].

The use of (27) is motivated by the following Proposition 2 which characterizes the discontinuity. The condition is next presented for the Prandtl–Reuss model with linear hardening and it is given in a more general format which applies to admissible solutions with jump across time instant t_n in the case of rate-independent plasticity.

Denote by

$$
s_{\text{ad}}(\mathbf{x}, t_n) = (\boldsymbol{\sigma}_{\text{ad}}(\mathbf{x}, t_n), R_{\text{ad}}(\mathbf{x}, t_n); \; \boldsymbol{\varepsilon}_{\text{ad}}(\mathbf{x}, t_n), \boldsymbol{\varepsilon}_{\text{ad}}^{\text{p}}(\mathbf{x}, t_n), p_{\text{ad}}(\mathbf{x}, t_n))
$$

and

$$s_{\mathrm{ad}}(\mathbf{x}, t_n + \Delta t) = (\boldsymbol{\sigma}_{\mathrm{ad}}(\mathbf{x}, t_n + \Delta t), R_{\mathrm{ad}}(\mathbf{x}, t_n + \Delta t);$$

$$\boldsymbol{\varepsilon}_{\mathrm{ad}}(\mathbf{x}, t_n + \Delta t), \boldsymbol{\varepsilon}_{\mathrm{ad}}^{\mathrm{p}}(\mathbf{x}, t_n + \Delta t), p_{\mathrm{ad}}(\mathbf{x}, t_n + \Delta t))$$

any admissible solution at t_n and $t_n + \Delta t$, respectively, corresponding to the same load level and with $s_{\mathrm{ad}}(t)$ the admissible solution obtained as time linear interpolation over $[t_n, t_n + \Delta t]$ of $s_{\mathrm{ad}}(t_n)$ and $s_{\mathrm{ad}}(t_n + \Delta t)$. We have then the following result [32]:

Proposition 2
Given the admissible solutions $s_{\mathrm{ad}}(t_n)$ and $s_{\mathrm{ad}}(t_n + \Delta t)$, corresponding to the same load level and meeting the finite value error requirements

$$\forall \mathbf{x} \in \Omega$$

$$\left| \begin{array}{l} (\boldsymbol{\sigma}_{\mathrm{ad}}(\mathbf{x}, t_n), R_{\mathrm{ad}}(\mathbf{x}, t_n)) \\[4pt] (\boldsymbol{\sigma}_{\mathrm{ad}}(\mathbf{x}, t_n + \Delta t), R_{\mathrm{ad}}(\mathbf{x}, t_n + \Delta t)) \end{array} \right. \in \mathbb{E}$$

$$p_{\mathrm{ad}}(\mathbf{x}, t_n + \Delta t) - p_{\mathrm{ad}}(\mathbf{x}, t_n) \geqslant \|\boldsymbol{\varepsilon}_{\mathrm{ad}}^{\mathrm{p}}(\mathbf{x}, t_n + \Delta t) - \boldsymbol{\varepsilon}_{\mathrm{ad}}^{\mathrm{p}}(\mathbf{x}, t_n)\|$$

$$\mathrm{Tr}(\boldsymbol{\varepsilon}_{\mathrm{ad}}^{\mathrm{p}}(\mathbf{x}, t_n + \Delta t) - \boldsymbol{\varepsilon}_{\mathrm{ad}}^{\mathrm{p}}(\mathbf{x}, t_n)) = 0$$

and not necessarily the state equations at t_n and $t_n + \Delta t$, respectively, it follows $\forall \mathbf{x} \in \Omega$,

$$\mathrm{IF} \left\{ \begin{array}{l} {}^{\mathrm{sl}}\eta_{\mathbf{x}, t_n}^2 = {}^{\mathrm{sl}}\eta_{\mathbf{x}, t_n + \Delta t}^2 = {}^{\mathrm{sl}}\eta_{\mathbf{x}, t}^2 \\[4pt] \forall t \in [t_n, t_n + \Delta t]. \\[4pt] {}^{\Delta}\zeta_{\mathbf{x}, d}^2(\mathbf{x}, t_n) = 0 \end{array} \right. \Rightarrow \left\{ \begin{array}{l} \boldsymbol{\sigma}_{\mathrm{ad}}(\mathbf{x}, t_n) = \boldsymbol{\sigma}_{\mathrm{ad}}(\mathbf{x}, t_n + \Delta t) \\[4pt] R_{\mathrm{ad}}(\mathbf{x}, t_n) = R_{\mathrm{ad}}(\mathbf{x}, t_n + \Delta t) \\[4pt] \boldsymbol{\varepsilon}_{\mathrm{ad}}(\mathbf{x}, t_n) = \boldsymbol{\varepsilon}_{\mathrm{ad}}(\mathbf{x}, t_n + \Delta t) \\[4pt] \boldsymbol{\varepsilon}_{\mathrm{ad}}^{\mathrm{p}}(\mathbf{x}, t_n) = \boldsymbol{\varepsilon}_{\mathrm{ad}}^{\mathrm{p}}(\mathbf{x}, t_n + \Delta t) \\[4pt] p_{\mathrm{ad}}(\mathbf{x}, t_n) = p_{\mathrm{ad}}(\mathbf{x}, t_n + \Delta t) \end{array} \right.$$

Proof
The proof is here only sketched. For more details we refer to Reference [32]. Time derivative of ${}^{\mathrm{sl}}\eta_{\mathbf{x}, t}^2$ delivers

$$\frac{\mathrm{d}}{\mathrm{d}t}\, {}^{\mathrm{sl}}\eta_{\mathbf{x}, t}^2 = 0 \Rightarrow \left| \begin{array}{l} \Delta\boldsymbol{\sigma}_{\mathrm{ad}} = \mathbf{C}\Delta\boldsymbol{\varepsilon}_{\mathrm{ad}}^{\mathrm{e}} \\[4pt] \Delta R_{\mathrm{ad}} = \mathsf{H}\Delta p_{\mathrm{ad}} \end{array} \right.$$

where we have let $\Delta(\bullet) = (\bullet)(\mathbf{x} + \Delta t) - (\bullet)(\mathbf{x}, t_n)$.

From the equilibrium at t_n and $t_n + \Delta t$ one has

$$\int_{\Omega} \Delta\boldsymbol{\sigma}_{\mathrm{ad}}: \ \Delta\boldsymbol{\varepsilon}_{\mathrm{ad}} \, \mathrm{d}\Omega = 0$$

The requirements for a finite value of the error along with the condition

$$^{\Delta}\zeta_d^2(\mathbf{x}, t_n) = R_0 \|\boldsymbol{\varepsilon}_{\mathrm{ad}}^{\mathrm{p}}(\mathbf{x}, t_n + \Delta t) - \boldsymbol{\varepsilon}_{\mathrm{ad}}^{\mathrm{p}}(\mathbf{x}, t_n)\|$$

$$- \frac{\boldsymbol{\sigma}_{\text{ad}}(\mathbf{x}, t_n + \Delta t) + \boldsymbol{\sigma}_{\text{ad}}(\mathbf{x}, t_n)}{2} : (\boldsymbol{\varepsilon}_{\text{ad}}^{\text{p}}(\mathbf{x}, t_n + \Delta t) - \boldsymbol{\varepsilon}_{\text{ad}}^{\text{p}}(\mathbf{x}, t_n))$$

$$+ \frac{R_{\text{ad}}(\mathbf{x}, t_n + \Delta t) + R_{\text{ad}}(\mathbf{x}, t_n)}{2} (p_{\text{ad}}(\mathbf{x}, t_n + \Delta t) - p_{\text{ad}}(\mathbf{x}, t_n)) = 0$$

give

$$\Delta\boldsymbol{\sigma}_{\text{ad}}: \ \Delta\boldsymbol{\varepsilon}_{\text{ad}}^{\text{p}} = \Delta R_{\text{ad}} \Delta p_{\text{ad}}$$

Therefore, it is

$$\int_{\Omega} \Delta\boldsymbol{\sigma}_{\text{ad}}: \ \Delta\boldsymbol{\varepsilon}_{\text{ad}}^{\text{e}} \, \mathrm{d}\Omega + \int_{\Omega} \Delta\boldsymbol{\sigma}_{\text{ad}}: \ \Delta\boldsymbol{\varepsilon}_{\text{ad}}^{\text{p}} \, \mathrm{d}\Omega = 0 \Leftrightarrow \int_{\Omega} \mathbf{C}\Delta\boldsymbol{\varepsilon}_{\text{ad}}^{\text{e}}: \ \Delta\boldsymbol{\varepsilon}_{\text{ad}}^{\text{e}} \, \mathrm{d}\Omega + \int_{\Omega} \mathsf{H}^2 \Delta p_{\text{ad}} \, \mathrm{d}\Omega = 0$$

$$\Leftrightarrow \left|
\begin{array}{l}
\Delta\boldsymbol{\varepsilon}_{\text{ad}}^{\text{e}} = 0 \Rightarrow \Delta\boldsymbol{\sigma}_{\text{ad}} = \mathbf{0} \\[2mm]
\Delta p_{\text{ad}} = 0 \Rightarrow \Delta R_{\text{ad}} = 0 \\[2mm]
\qquad \overset{(a)}{\Rightarrow} \Delta\boldsymbol{\varepsilon}_{\text{ad}}^{\text{p}} = \mathbf{0}
\end{array}
\right.$$

where implication (a) follows from the conditions imposed on the admissible solution to deliver a finite value of the error.

4.3. Definition of error in solution

Let

$$s_{\text{ad}}^{\text{kin}}(\mathbf{x}, t) = (\mathbf{u}_{\text{ad}}(\mathbf{x}, t), \boldsymbol{\varepsilon}_{\text{ad}}^{\text{p}}(\mathbf{x}, t), \boldsymbol{\alpha}_{\text{ad}}(\mathbf{x}, t), p_{\text{ad}}(\mathbf{x}, t)) \tag{28}$$

denote a kinematically admissible solution with $\mathbf{u}$ meeting the compatibility conditions, and $\boldsymbol{\varepsilon}_{\text{ad}}^{\text{p}}(\mathbf{x}, t), \boldsymbol{\alpha}_{\text{ad}}(\mathbf{x}, t), p_{\text{ad}}(\mathbf{x}, t)$ meeting the initial conditions. The kinematically admissible solution may also present discontinuity jump across time instants t_n. We assume the error in the constitutive equations produced by

$$s_{\text{ex,ad}} = (\boldsymbol{\sigma}_{\text{ex}}, \mathbf{X}_{\text{ex}}, R_{\text{ex}}; \mathbf{u}_{\text{ad}}, \boldsymbol{\varepsilon}_{\text{ad}}^{\text{p}}, \boldsymbol{\alpha}_{\text{ad}}, p_{\text{ad}})$$

as global measure of the exact error in solution associated with $s_{\text{ad}}^{\text{kin}}$. This is defined as

$$e_{\text{ex}}^2(T) = \sup_{t \leqslant T} \theta_{\text{ex}}^2(t) \tag{29}$$

where

$$\theta_{\text{ex}}^2(t) = 2 \int_{\Omega} {}^{\text{sl}}\eta_{\mathbf{x}, t}^2(\boldsymbol{\sigma}_{\text{ex}}, \mathbf{X}_{\text{ex}}, R_{\text{ex}}; \ \boldsymbol{\varepsilon}_{\text{ad}}^{\text{p}}, \boldsymbol{\alpha}_{\text{ad}}, p_{\text{ad}}) \, \mathrm{d}\Omega\big|_t$$

$$+ 2 \int_{\Omega} \int_0^t {}^{\text{d}}\eta_{\mathbf{x}, \tau}^2(\boldsymbol{\sigma}_{\text{ex}}, \mathbf{X}_{\text{ex}}, R_{\text{ex}}; \ \dot{\boldsymbol{\varepsilon}}_{\text{ad}}^{\text{p}}, \dot{\boldsymbol{\alpha}}_{\text{ad}}, \dot{p}_{\text{ad}}) \, \mathrm{d}\tau \, \mathrm{d}\Omega$$

This definition of error is meaningful, in the sense that it can easily be shown [32] that $e_{\text{ex}}^2(T) = 0$ if and only if $s_{\text{ex,ad}}$ is time continuous and $s_{\text{ex,ad}}(\mathbf{x}, t) = s_{\text{ex}}(\mathbf{x}, t)$, $\forall \mathbf{x} \in \Omega$, $\forall t \leqslant T$. Also, by employing the extension of the Prager–Synge theorem given in Reference [23], the following bound can be proved [32]

$$e_{\text{ex}} \leqslant e_{\text{dis}}$$

where e_{dis} is the dissipation error [13], that is, the error in the constitutive equations produced by an admissible solution that meets also the state laws.

5. FINITE ELEMENT SOLUTION WITH CHANGE OF MESH AT t_n. TRANSFER PROCEDURES

We consider next the conforming displacement finite element solution of the nonlinear incremental boundary value problem obtained by the backward Euler time integration scheme.

Let $0 = t_1 < \cdots < t_n < \cdots < t_{N+1} = T$ be a partition of the time interval of interest $[0, T]$ and set $k_n = t_{n+1} - t_n$. Denote with $\Omega_l^{h_{n+1}} \in \mathscr{T}_{h_{n+1}}$ a generic element of the triangulation $\mathscr{T}_{h_{n+1}}$ and with $\mathbf{x}_{l,j}^{h_{n+1}} \in \Omega_l^{h_{n+1}}$ the jth Gauss point of the element $\Omega_l^{h_{n+1}}$ and ngp its number.

The fully discrete problem relative to the time interval $[t_n, t_{n+1}]$, formulated with generic data $\tilde{\boldsymbol{\varepsilon}}_n^{\text{p}}(\mathbf{x}), \tilde{\boldsymbol{\alpha}}_n(\mathbf{x})$, reads as

Given: $\quad \forall \Omega_l^{h_{n+1}} \in \mathscr{T}_{h_{n+1}}$ and for $j = 1, \ldots, ngp$,

External Loading $\qquad\qquad\qquad\qquad \mathbf{b}_{n+1}(\mathbf{x}_{l,j}^{h_{n+1}})$

State of the system at t_n $\qquad\qquad\quad \begin{vmatrix} \tilde{\boldsymbol{\varepsilon}}_n^{\text{p}}(\mathbf{x}_{l,j}^{h_{n+1}}) \\ \tilde{\boldsymbol{\alpha}}_n(\mathbf{x}_{l,j}^{h_{n+1}}) \end{vmatrix}$ $\qquad\qquad\qquad$ (30)

Find: $\quad \mathbf{u}_{n+1}^{h_{n+1}}(\mathbf{x}) \in \mathscr{V}^{h_{n+1}}$

Such that: $\displaystyle \sum_{\Omega_l^{h_{n+1}} \in \mathscr{T}_{h_{n+1}}} \sum_{j=1}^{ngp} j_{l,j} w_{l,j} \left\{ {}^{h_{n+1}}\boldsymbol{\sigma}_{n+1}(\mathbf{x}_{l,j}^{h_{n+1}}) : \nabla \boldsymbol{\eta}^{h_{n+1}}(\mathbf{x}_{l,j}^{h_{n+1}}) \right.$

$\left. \qquad - \mathbf{b}_{n+1}(\mathbf{x}_{l,j}^{h_{n+1}}) : \boldsymbol{\eta}^{h_{n+1}}(\mathbf{x}_{l,j}^{h_{n+1}}) \right\} = 0, \quad \forall \boldsymbol{\eta}^{h_{n+1}} \in \mathscr{V}_0^{h_{n+1}}$

where the stress tensor ${}^{h_{n+1}}\boldsymbol{\sigma}_{n+1}(\mathbf{x}_{l,j}^{h_{n+1}})$ is obtained by solving at $\mathbf{x}_{l,j}^{h_{n+1}}$ the constitutive incremental problem with data $\tilde{\boldsymbol{\varepsilon}}_n^{\text{p}}(\mathbf{x}_{l,j}^{h_{n+1}})$, $\tilde{\boldsymbol{\alpha}}_n(\mathbf{x}_{l,j}^{h_{n+1}})$ and prescribed strain $\boldsymbol{\varepsilon}_{n+1}^{h_{n+1}}(\mathbf{x}_{l,j}^{h_{n+1}}) = \nabla_s \mathbf{u}_{n+1}^{h_{n+1}}(\mathbf{x}_{l,j}^{h_{n+1}})$. The constitutive incremental problem (CInP) is obtained by applying the backward Euler time discretization scheme to the solution of the initial value constitutive problem described in Box 1. In Equation (30) $w_{l,j}$ and $j_{l,j}$ denote the weight and the value of the Jacobian determinant at the Gauss point $\mathbf{x}_{l,j}$ [34]. For the sake of notation, the work of the traction forces in (30) has been dropped.

The choice of the quantities in rate form as secondary variables and the use of backward Euler as time discrete scheme poses, however, the question on how to define the data $\tilde{\boldsymbol{\varepsilon}}_n^{\text{p}}(\mathbf{x}_{l,j}^{h_{n+1}})$ and $\tilde{\boldsymbol{\alpha}}_n(\mathbf{x}_{l,j}^{h_{n+1}})$ for problem (30) in the case the finite element mesh adopted for its discretization

is different from the one used in the previous time interval. In this case, inasmuch as the mesh changes across the time node t_n, the Gauss points change as well and it is no more possible to define the history of the secondary variables at these points if they have not been considered from the initial time $t = 0$.

The procedures currently in use for the definition of these data, in general, try to compute the value of the unknowns fields $\tilde{\varepsilon}_n^{\mathrm{p}}(\mathbf{x}_{l,j}^{h_{n+1}})$, $\tilde{\alpha}_n(\mathbf{x}_{l,j}^{h_{n+1}})$ at the new integration points, $\mathbf{x}_{l,j}^{h_{n+1}} \in \Omega_l^{h_{n+1}}$ with $\Omega_l^{h_{n+1}} \in \mathscr{T}_{h_{n+1}}$, in terms of the values ${}^{h_n}\varepsilon_n^{\mathrm{p}}(\mathbf{x}_{\mathrm{e},i}^{h_n})$, ${}^{h_n}\alpha(\mathbf{x}_{\mathrm{e},i}^{h_n})$, solution relative to the previous time interval $[t_{n-1}, t_n]$ at the old integration points, $\mathbf{x}_{\mathrm{e},i}^{h_n} \in \Omega_{\mathrm{e}}^{h_n}$ with $\Omega_{\mathrm{e}}^{h_n} \in \mathscr{T}_{h_n}$.

These procedures are usually known by the name of Transfer of Data. Though it appears difficult trying to draw a classification, the fundamental approaches and ideas can be referred to the following procedures [32]:

- Variationally consistent transfer.
- Weak enforcement continuity transfer.
- Smoothing transfer.

These transfer processes are in the following presented with reference to the specific problem at hand. This means that only transfer of ε^{p} and α will be analysed. It is also worth noting that all the following operations share the same underlying idea of defining first a field for the state variables which depends on the old mesh with its relative distribution of the elemental Gauss points. This field is then transformed, according to the specific procedure, into a new field on the new mesh which allows the sampling at the new Gauss points. The resulting function is denoted by $(\tilde{\bullet})_n$. The latter is equilibrated with respect to the new mesh by delivering ${}^{h_{n+1}}(\bullet)_n$. The difference between the two fields, ${}^{h_n}(\bullet)_n - {}^{h_{n+1}}(\bullet)_n$, defines the discontinuity.

5.1. Variationally consistent transfer

This class of transfers has been analysed by Ortiz and coworkers in References [3, 35, 36]. A variationally consistent transfer is a remapping procedure where the initial data is obtained from sampling at new Gauss points the solution of the variational formulation of the incremental boundary value problem for the time step $[t_{n-1}, t_n]$. For this to happen, the equations that define the secondary variables, and appearing as data of the problem, must be expressed in a variational form and consequently an interpolation for those variables must be prescribed. It is this variational formulation that provides the data for the fully discrete problem in case of change of mesh. This observation, therefore, suggests enforcement of the CInNP in a weak form and not in a pointwise manner, as it is implied by the standard displacement formulation. However, inasmuch as we are interested to perform transfer of the variables obtained from the displacement formulation, we must ensure that the solution obtained from this more general variational formulation conforms to the one obtained from the displacement formulation.

This can easily be achieved, as it is asserted in Reference [3], by an appropriate choice of the interpolation functions for the secondary variables and assuming the same element-base quadrature scheme. Since the fields $\sigma(\mathbf{x})$, $\varepsilon^{\mathrm{p}}(\mathbf{x})$, $\alpha(\mathbf{x})$ are not involved in spatial derivative in the general variational formulation, unlike the displacement field $\mathbf{u}(\mathbf{x})$, the respective finite element interpolation functions are not required to be continuous over the element and across the element boundaries [3] but only to meet general regularity properties. This allows the variational equations of the constitutive equations to be imposed element by element.
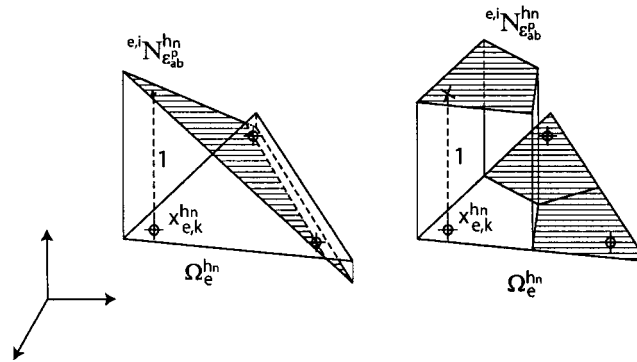
Figure 1. Possible choices for the interpolation functions of the internal variables which comply with the requirements of Equation (32).

Furthermore, if we assume the values of the field at the quadrature points as degrees of freedom for the element interpolant of the state variable, then the Galerkin finite element approximation becomes equivalent to the set of equations that enforce the constitutive equations at each Gauss point of the element. This equivalence of the displacement formulation based on element quadrature with underlying more general variational formulations represents an example of limitation principle introduced by Reference [37] for mixed formulations.

It can easily be shown [32] that the displacement formulation of the incremental boundary value problem for the time step $[t_{n-1}, t_n]$ can be obtained from an underlying more general variational formulation of the same incremental boundary value problem. This formulation presents also ε^p and α as independent variables with the following interpolation assumptions holding over each element for their components $(\varepsilon^p)_{a,b}$ and $(\alpha^p)_{c,d}$, respectively

$$\left|\begin{array}{l} ({}^e\varepsilon_n^{p,h_n})_{a,b}(\mathbf{x}) = \sum_{i=1}^{ngp} {}^{e,i}\mathbb{N}^{h_n}_{(\varepsilon^p)_{a,b}}(\mathbf{x})({}^{e,i}\bar\varepsilon_n^{p^{h_n}})_{a,b} \\ ({}^e\alpha_n^{h_n})_{c,d}(\mathbf{x}) = \sum_{i=1}^{ngp} {}^{e,i}\mathbb{N}^{h_n}_{(\alpha)_{c,d}}(\mathbf{x})({}^{e,i}\bar\alpha_n^{h_n})_{c,d} \end{array}\right. \tag{31}$$

with the elemental shape functions being piecewise continuous and meeting the following requirements:

$$\left|\begin{array}{l} {}^{e,i}\mathbb{N}^{h_n}_{(\varepsilon^p)_{a,b}}(\mathbf{x}^{h_n}_{e,k}) = \delta_{i,k} \\ {}^{e,i}\mathbb{N}^{h_n}_{(\alpha)_{a,b}}(\mathbf{x}^{h_n}_{e,k}) = \delta_{i,k} \end{array}\right. \tag{32}$$

In Equation (32) $\delta_{i,k}$ is the Kronecker symbol whereas in Equation (31) the coefficients $({}^{e,i}(\bar\bullet)_{n+1}^{h_{n+1}})_{a,b}$ identify with the value of the component of the respective field at the Gauss points $\mathbf{x}^{h_n}_{e,i}$. The latter results from the displacement finite element solution at t_n.

Figure 1 depicts some possible choices for ${}^{e,i}\mathbb{N}^{h_n}_{\varepsilon^p_{ab}}$, for example, where ε^p_{ab} denotes a component of the second order tensor ε^p.

$$(\bullet)(x_{e,i}^{h_n}) \xrightarrow{\text{(a)}} {}_{e,i}(\bullet)(x_N^{h_n}) \xrightarrow{\text{(b)}} (\bullet)(x_N^{h_n}) \xrightarrow{\text{(c)}} (\bullet)(x^{h_n}) \xrightarrow{\text{(d)}}$$

$$\xrightarrow{\text{(d)}} (\bullet)(x^{h_{n+1}}) = \mathcal{I}^{\mathcal{V}^{h_{n+1}}} (\bullet)(x^{h_n}) \xrightarrow{\text{(e)}} (\bullet)(x_{l,j}^{h_{n+1}})$$

Figure 2. Smoothing transfer: (a) extrapolation of Gauss points values to the nodes of old mesh; (b) averaging at the nodes of old mesh; (c) finite element interpolation on old mesh; (d) nodal interpolation onto new mesh; and (e) sampling at new Gauss points.

Finally, the state of the system at t_n^+, that is, $\tilde{\varepsilon}_n^p(\mathbf{x}_{l,j}^{h_{n+1}})$ and $\tilde{\boldsymbol{\alpha}}_n(\mathbf{x}_{l,j}^{h_{n+1}})$, is obtained by sampling the fields (31) at the new Gauss points $x_{l,j}^{h_{n+1}} \in \Omega_l^{h_{n+1}}$.

5.2. Weak enforcement continuity transfer

This transfer procedure is obtained from an approximation *a la* Galerkin of the variational equation which imposes in the weak form the continuity across the time node t_n of the variables which appear as data of the InBVP.

Let us assume, in the following, as general regularity property that $(\tilde{\bullet})_n \in (L^2(\Omega))^{n_{\dim}}$ and also that $(\bullet)_n \in (L^2(\Omega))^{n_{\dim}}$, with $n_{\dim}$ equal to the number of components of the respective tensor field with respect to a given basis. The field $(\tilde{\bullet})_n$ is the data for the InBVP whereas $(\bullet)_n$ is relative to the solution at the previous time interval.

The following condition

$$\langle (\tilde{\bullet})_n - (\bullet)_n, \boldsymbol{\theta} \rangle = 0, \quad \forall \boldsymbol{\theta} \in (L^2(\Omega))^{n_{\dim}} \tag{33}$$

enforces, in the weak form, the continuity of the field $(\bullet)_n$ across the time node t_n with $\langle \bullet, \bullet \rangle$ being an inner product in the space $(L^2(\Omega))^{n_{\dim}}$.

In Reference [22], condition (33) is enforced in a Galerkin sense by replacing the infinite dimensional space $(L^2(\Omega))^{n_{\dim}}$ with finite dimensional spaces. These are defined by piecewise constant functions representing the distribution assumption for the variables ε_n^p and $\boldsymbol{\alpha}_n^p$ and corresponding to the two triangulations $\mathscr{T}_{h_n}$, and $\mathscr{T}_{h_{n+1}}$, respectively.

5.3. Smoothing transfer

This procedure represents perhaps the most widely used remapping algorithm in solid mechanics applications for its relatively simple implementation. Details on the transfer operation can be found in References [21, 38]. The main steps are summarized in Figure 2. The values of the state variables $(\bullet)$ at the old Gauss points, $(\bullet)(\mathbf{x}_{e,i}^{h_n})$, are first transferred to the nodes of the old mesh, ${}_{e,i}(\bullet)(\mathbf{x}_N^{h_n})$, possibly also with some weighting. A weighted average is then carried out at each node, $(\bullet)(\mathbf{x}_N^{h_n})$, and a smooth field, $(\bullet)(\mathbf{x}^{h_n})$, is consequently defined by interpolation of the nodal values by means of the basis functions of the finite element space, $\mathscr{V}^{h_n}$, associated with the old mesh. The nodal interpolant of this field with respect to the new finite element space, $(\bullet)(\mathbf{x}^{h_{n+1}}) = \mathscr{I}^{\mathscr{V}^{h_{n+1}}}(\bullet)(\mathbf{x}^{h_n})$, is constructed and the resulting field is sampled at the new Gauss points delivering therein the transferred values of the state variables, $(\bullet)(\mathbf{x}_{l,j}^{h_{n+1}})$.

Some of the above steps can be by-passed and each of them can be executed in different ways, delivering a fairly large spectrum of transfer procedures.

5.4. Augmented extended dissipation error

The finite element solution obtained by the displacement formulation described in the previous section, is not in general an admissible solution. The finite element stresses do not satisfy the equilibrium equations in a pointwise manner.

In order to apply the theory of the error in the constitutive equations, given the finite element solution, an admissible solution that is as close as possible to the given finite element solution needs to be defined so that it can mirror all the approximations affecting the finite element solution [30].

Furthermore, consistently with an assumed linear variation of the external load over each time interval, and the convexity of the equilibrium and compatibility conditions, the admissible solution is taken to vary linearly over $[t_n, t_{n+1}]$. Therefore for its complete definition we need to solve the following problem:

$$\text{Given:} \quad \text{the admissible solution at } t_n,$$

$$\text{the finite element solution at } t_{n+1},$$

$$\text{Find:} \quad \text{a corresponding admissible solution at } t_{n+1}.$$

Next, we present first the construction in the case of constant finite element mesh. The case of change of mesh will then result as a special case of this procedure.

5.4.1. Construction of an admissible solution.

In the definition of an admissible solution for the computation of the extended dissipation error, the statically admissible variables are not constrained to their conjugate variables by means of the state laws. This allows more information from the finite element solution to be included in building the corresponding admissible solution and strengthen the link between the two solutions. For instance, in the case of the J_2-plasticity model and in the case of finite element solution which delivers plastic strains meeting the incompressibility condition, the computed plastic strain field can be assumed, in some circumstances which will be clarified next, as part of the admissible solution. In particular, the plastic strain, known only at the Gauss points $\mathbf{x}_{e,i}^h$ of the element used for the numerical integration of the constitutive equations, can be extended over the element to a field $^h\boldsymbol{\varepsilon}_{n+1}^p(\mathbf{x})$ which continues to meet the incompressibility condition. This can be realized, for example, by assuming each element partitioned by the Voronoi cells associated with each Gauss point and assuming a constant distribution of the plastic strain over the cell equal to the value of the strain at the respective Gauss point, cf. Figure 3.

Likewise, conforming finite element displacements can be used as part of the admissible solution and do not need to be modified, in contrast to the definition of the admissible solution used in computation of the dissipation error [39].

A key feature of the analysis and implementation of the error in the constitutive equations, however, is the definition of an equilibrated stress field $\boldsymbol{\sigma}_{ad}(\mathbf{x}, t_{n+1})$ linked to the finite element solution $^h\boldsymbol{\sigma}_{n+1}(\mathbf{x}_{e,i}^h)$. In the sequel we refer to the techniques initiated by Reference [11] where the so called prolongation condition depending in general on the regularity of the mesh establishes the aforementioned link [30]. In particular, hereafter, we apply the strong prolongation condition as introduced and analysed in References [11, 30, 40]. This condition distinguishes the statically admissible stress fields $\boldsymbol{\sigma}_{ad}(\mathbf{x}, t_{n+1})$ which satisfy the following
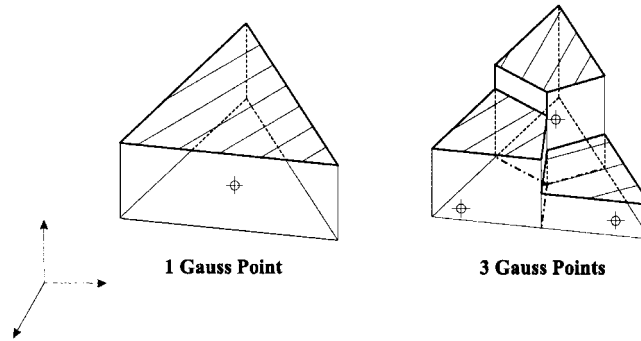
Figure 3. Partition of a triangular element with Voronoi cells relative to its Gauss points along with respective assumed distribution for the internal variables.

equation for every shape function $\mathbb{N}_i(\mathbf{x})$ and for all the elements Ω_e,

$$\int_{\Omega_e} \left(\boldsymbol{\sigma}_{ad}(\mathbf{x}, t_{n+1}) - {}^h\boldsymbol{\sigma}_{n+1}(\mathbf{x}) \right) : \nabla \mathbb{N}_i(\mathbf{x}) \, d\Omega = 0 \tag{34}$$

The only unknowns left apart and necessary to determine a complete admissible solution are, therefore,

$$\boldsymbol{\varepsilon}_{ad}^p(\mathbf{x}, t_{n+1}), \, p_{ad}(\mathbf{x}, t_{n+1}), \, \boldsymbol{\alpha}_{ad}(\mathbf{x}, t_{n+1})$$

$$R_{ad}(\mathbf{x}, t_{n+1}), \, \mathbf{X}_{ad}(\mathbf{x}, t_{n+1})$$

For their computation, the general method of minimization of the error introduced in Reference [14] can be adopted. The minimization can he carried out at each point of the domain since there are no spatial derivative involved in the constitutive equations, in particular it can be done at the Gauss points used to compute numerically the space integrals that define the error [30]. These quadrature points do not have to be confused with those used for the numerical integration of the constitutive equations, which in turn are the one used to compute numerically the integral that appear in the internal virtual power.

However, in general, it may be much more convenient to resort to the simpler criterion given in Reference [39] which resembles the integration of the evolution law for the constitutive model which is used. Next, we detail the definition of the admissible state variables $R_{ad}(\mathbf{x}, t_{n+1})$, $\boldsymbol{\varepsilon}_{ad}^p(\mathbf{x}, t_{n+1})$, $p_{ad}(\mathbf{x}, t_{n+1})$ in the case of the Prandtl–Reuss model.

The admissible thermodynamic force $R_{ad}(\mathbf{x}, t_{n+1})$ is assumed as

$$R_{ad}(\mathbf{x}, t_{n+1}) = \text{Max}\{R_1, R_2\}$$

where

$$R_1 = \|\boldsymbol{\sigma}_{ad}^D(\mathbf{x}, t_{n+1})\| - R_0 \quad \text{and} \quad R_2 = R_{ad}(\mathbf{x}, t_n)$$

The admissible plastic strain, on the other hand, will be given by

$$\boldsymbol{\varepsilon}_{ad}^p(\mathbf{x}, t_{n+1}) = {}^h\boldsymbol{\varepsilon}_{n+1}^p(\mathbf{x})$$

if the following condition is satisfied:

$$\boldsymbol{\sigma}_{\text{ad}}(\mathbf{x}, t_{n+1}) : [{}^{h}\boldsymbol{\varepsilon}_{n+1}^{\text{p}}(\mathbf{x}) - \boldsymbol{\varepsilon}_{\text{ad}}^{\text{p}}(\mathbf{x}, t_{n})] \geqslant 0 \qquad (35)$$

otherwise we choose

$$\boldsymbol{\varepsilon}_{\text{ad}}^{\text{p}}(\mathbf{x}, t_{n+1}) = \boldsymbol{\varepsilon}_{\text{ad}}^{\text{p}}(\mathbf{x}, t_{n})$$

Finally, with regard to the admissible accumulated plastic strain $p_{\text{ad}}(\mathbf{x}, t_{n+1})$ it is

$$p_{\text{ad}}(\mathbf{x}, t_{n+1}) = p_{\text{ad}}(\mathbf{x}, t_{n}) + \|\boldsymbol{\varepsilon}_{\text{ad}}^{\text{p}}(\mathbf{x}, t_{n+1}) - \boldsymbol{\varepsilon}_{\text{ad}}^{\text{p}}(\mathbf{x}, t_{n})\|$$

which corresponds to the integration of the equation $\dot{p} = \|\dot{\boldsymbol{\varepsilon}}_{\text{ad}}^{\text{p}}\|$ that occurs for the model under consideration by assuming linear variation of the variables over $[t_{n}, t_{n+1}]$.

Condition (35), which represents the discrete implicit expression of the plastic power, can be interpreted in the light of a constrained minimization of the pointwise contribution to the error in the evolution law, θ_{d}^{2}, within the time interval $[t_{n}, t_{n+1}]$ [32].

In the case of change of finite element mesh at the time instant t_{n}, the aforementioned criteria can also be used to define the admissible solution corresponding to the finite element solution at t_{n}^{+}, provided that one replaces t_{n+1} with t_{n}^{+}. The general procedure is summarized in Box 2 whereas Figure 4 depicts schematically the notation relative to the finite element solutions and corresponding admissible solutions.

Remark 5.1
In order to define an admissible solution, a hypothesis on the distribution over each element of the state variables, which are obtained from the finite element solution at t_{n}^{+} at the Gauss points of the new mesh, must be made. Hereafter, we refer to the distributions depicted in Figure 3. As a result, the error in the constitutive equations must be considered as the error associated with this given postulation for the variables distribution. This in turn allows for the definition of the discontinuity of the fields across the time node t_{n}.

Remark 5.2
The admissible solution at t_{n}^{-} is known at the Gauss points of the old mesh, which are employed to compute numerically the space integrals that define the error at t_{n}^{-}. The element based quadrature of the space integrals that define the error at t_{n}^{+}, on the other hand, requires the knowledge of the admissible solution at t_{n}^{+} at the quadrature points of the new mesh. In order to implement the procedure shown in Box 2, the values of the fields $\boldsymbol{\varepsilon}_{\text{ad}}^{\text{p}}(\mathbf{x}, t_{n}^{-})$ and $p_{\text{ad}}(\mathbf{x}, t_{n}^{-})$ at the quadrature points of the new mesh are necessary. These are simply obtained by suitable interpolation of their values at the Gauss points of the old mesh.

Remark 5.3
The statically admissible stress fields $\boldsymbol{\sigma}_{\text{ad}}(\mathbf{x}, t_{n}^{-})$ and $\boldsymbol{\sigma}_{\text{ad}}(\mathbf{x}, t_{n}^{+})$ correspond to the same load level but they are defined as prolongation of different finite element stresses.

For convenience we recall the expression of the augmented extended dissipation error by highlighting the terms due to the change of mesh and the different contributions to the error

Box 2. Procedure to build an admissible solution at t_n^+ in the presence of change of mesh.

DATA:

Admissible solution at t_n^- $\quad\left|\begin{array}{l}\boldsymbol{\sigma}_{\mathrm{ad}}(\mathbf{x}, t_n^-), \ R_{\mathrm{ad}}(\mathbf{x}, t_n^-) \\ \boldsymbol{\varepsilon}_{\mathrm{ad}}(\mathbf{x}, t_n^-), \ \boldsymbol{\varepsilon}_{\mathrm{ad}}^{\mathrm{p}}(\mathbf{x}, t_n^-), \ p_{\mathrm{ad}}(\mathbf{x}, t_n^-)\end{array}\right.$

Finite element solution at t_n^+ $\quad\left|\begin{array}{l}\mathbf{u}_n^{h_{n+1}}(\mathbf{x}), \ \boldsymbol{\varepsilon}_n^{h_{n+1}}(\mathbf{x}) = \nabla_s \mathbf{u}_n^{h_{n+1}}(\mathbf{x}) \\ {}^{h_{n+1}}\boldsymbol{\varepsilon}_n^{\mathrm{p}}(\mathbf{x}), \ {}^{h_{n+1}} p_n(\mathbf{x}), \ {}^{h_{n+1}}\boldsymbol{\sigma}_n(\mathbf{x})\end{array}\right.$

FIND:

Admissible solution at t_n^+ $\quad\left|\begin{array}{l}\boldsymbol{\sigma}_{\mathrm{ad}}(\mathbf{x}, t_n^+), \ R_{\mathrm{ad}}(\mathbf{x}, t_n^+) \\ \boldsymbol{\varepsilon}_{\mathrm{ad}}(\mathbf{x}, t_n^+), \ \boldsymbol{\varepsilon}_{\mathrm{ad}}^{\mathrm{p}}(\mathbf{x}, t_n^+), \ p_{\mathrm{ad}}(\mathbf{x}, t_n^+)\end{array}\right.$

WHERE

Admissible generalised stress field at t_n^+ :

$\boldsymbol{\sigma}_{\mathrm{ad}}(\mathbf{x}, t_n^+), R_{\mathrm{ad}}(\mathbf{x}, t_n^+)$

$\left|\begin{array}{l}\displaystyle\int_\Omega \boldsymbol{\sigma}_{\mathrm{ad}}(\mathbf{x}, t_n^+) : \nabla\boldsymbol{\eta}(\mathbf{x})\,\mathrm{d}\Omega = \int_\Omega \mathbf{b}_n(\mathbf{x})\boldsymbol{\eta}(\mathbf{x})\,\mathrm{d}\Omega + \int_{\partial\Omega_1} \mathbf{t}_n(\mathbf{x})\boldsymbol{\eta}(\mathbf{x})\,\mathrm{d}s, \ \ \forall\boldsymbol{\eta} \in \mathscr{V}_0 \\[6pt] \forall\Omega_e^{h_{n+1}} \in \mathscr{T}_{h_{n+1}}, \qquad \displaystyle\int_{\Omega_e^{h_{n+1}}} [\boldsymbol{\sigma}_{\mathrm{ad}}(\mathbf{x}, t_n^+) - {}^{h_{n+1}}\boldsymbol{\sigma}_n(\mathbf{x})] : \nabla\mathbb{N}_i\,\mathrm{d}\Omega = 0 \\[2pt] \forall\mathbb{N}_i, \ \forall \text{ vertex nodes } i \\[4pt] R_{\mathrm{ad}} = \max\{R_1, R_2\} \\[4pt] \text{where } R_1 = \|\boldsymbol{\sigma}_{\mathrm{ad}}^D(\mathbf{x}, t_n^+)\| - R_0 \\[4pt] \qquad\quad R_2 = R_{\mathrm{ad}}(\mathbf{x}, t_n^-)\end{array}\right.$

Admissible kinematic solution at t_n^+ :

$\boldsymbol{\varepsilon}_{\mathrm{ad}}(\mathbf{x}, t_n^+)$,

$\boldsymbol{\varepsilon}_{\mathrm{ad}}^{\mathrm{p}}(\mathbf{x}, t_n^+), p_{\mathrm{ad}}(\mathbf{x}, t_n^+)$

$\left|\begin{array}{l}\mathbf{u}_{\mathrm{ad}}(\mathbf{x}, t_n^+) = \mathbf{u}_n^{h_{n+1}}(\mathbf{x}), \ \ \boldsymbol{\varepsilon}_{\mathrm{ad}}(\mathbf{x}, t_n^+) = \nabla_s \mathbf{u}_{\mathrm{ad}}(\mathbf{x}, t_n^+) \\[4pt] \text{IF } \ \boldsymbol{\sigma}_{\mathrm{ad}}(\mathbf{x}, t_n^+) : [{}^{h_{n+1}}\boldsymbol{\varepsilon}_n^{\mathrm{p}}(\mathbf{x}) - \boldsymbol{\varepsilon}_{\mathrm{ad}}^{\mathrm{p}}(\mathbf{x}, t_n^-)] \geqslant 0 \\[4pt] \quad \boldsymbol{\varepsilon}_{\mathrm{ad}}^{\mathrm{p}}(\mathbf{x}, t_n^+) = {}^{h_{n+1}}\boldsymbol{\varepsilon}_n^{\mathrm{p}}(\mathbf{x}) \\[4pt] \text{ELSE} \\[4pt] \quad \boldsymbol{\varepsilon}_{\mathrm{ad}}^{\mathrm{p}}(\mathbf{x}, t_n^+) = \boldsymbol{\varepsilon}_{\mathrm{ad}}^{\mathrm{p}}(\mathbf{x}, t_n^-) \\[4pt] \text{END IF} \\[4pt] p_{\mathrm{ad}}^{\mathrm{p}}(\mathbf{x}, t_n^+) = p_{\mathrm{ad}}(\mathbf{x}, t_n^-) + \|\boldsymbol{\varepsilon}_{\mathrm{ad}}^{\mathrm{p}}(\mathbf{x}, t_n^+) - \boldsymbol{\varepsilon}_{\mathrm{ad}}^{\mathrm{p}}(\mathbf{x}, t_n^-)\|\end{array}\right.$

from the parts of the admissible solution which are continuous in time

$$
e_{\mathrm{ext}}^{n,c\,2}(T) = \mathrm{MAX}\Bigg\{ \sup_{t \leqslant t_n^-}\Bigg[\overbrace{\underbrace{2\int_\Omega {}^{\mathrm{sl}}\eta_{\mathbf{x},t}^2\,\mathrm{d}\Omega}_{\theta_{\mathrm{sl}}^{o\,2}(t)} + \underbrace{2\int_\Omega\int_0^t {}^d\eta_{\mathbf{x},\tau}^2\,\mathrm{d}\tau\,\mathrm{d}\Omega}_{\theta_d^{o\,2}(t)}}^{e_{\mathrm{ext}}^{o\,2}(t_n^-)}\Bigg],
$$

$$
\underbrace{\hspace{15em}}_{\theta^{o\,2}(t)}
$$

$$
\sup_{t_n^+ \leqslant t \leqslant T}\Bigg[\underbrace{2\int_\Omega {}^{\mathrm{sl}}\eta_{\mathbf{x},t}^2\,\mathrm{d}\Omega}_{\theta_{\mathrm{sl}}^{n,c\,2}(t)} + \theta_d^{o\,2}(t_n^-) + \underbrace{2\int_\Omega {}^\Delta\zeta_d^2(\mathbf{x}, t_n)\,\mathrm{d}\Omega}_{\Delta\theta_d^2(t_n)} + \underbrace{2\int_\Omega\int_{t_n^+}^t {}^d\eta_{\mathbf{x},\tau}^2\,\mathrm{d}\tau\,\mathrm{d}\Omega}_{[t_n^+,t]\theta_d^{n,c\,2}}\Bigg]\Bigg\}
$$

$$
\underbrace{\hspace{20em}}_{\theta^{n,c\,2}(t)}
$$

(36)

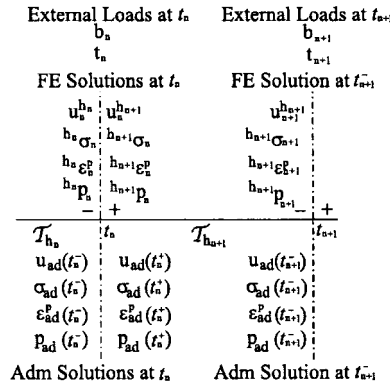Figure 4. Finite element solutions and admissible solutions for change of finite element mesh $\mathcal{T}_{h_n} \to \mathcal{T}_{h_{n+1}}$ at the time instant t_n.

In Equation (36), the notation $e_{\text{ext}}^{n,c^2}(T)$ has been adopted in place of $^\Delta e_{\text{ext}}^2(T)$ used in Equation (26). Here, the superscripts 'o' and 'n, c' stand for old and new mesh (after change), respectively.

In (36) we can distinguish primarily two terms. One, θ_d^2, is related to the history of the variables by means of an L^1 accumulation in time of the error in the evolution law, whereas the other term, θ_{sl}^2, depends on the current value of the error in the state law. As a result, following the change of a mesh, only the term θ_{sl}^2 can be reduced whereas the term θ_d^2 increases by at least the quantity $^\Delta\theta_d^2$. Therefore, there is an immediate advantage to change mesh for given definition of the initial data if at least the following inequality is satisfied:

$$\theta_{\text{sl}}^{o^2}(t_n^-) \geqslant \theta_{\text{sl}}^{n,c^2}(t_n^+) + {}^\Delta\theta_d^2(t_n) \tag{37}$$

The occurrence of (37) guarantees that $\theta^{n,c}(t_n^+) \leqslant e_{\text{ext}}^o(t_n^-)$

Remark 5.4
There will be no convenience to change mesh if the error associated with the evolution law, which is the error component that cannot be reduced for being associated with the quality of the solution up to the current time t_n, assumes values close to the prescribed global tolerance, that is, if the error associated with the past history of the solution has been significant. This circumstance would indicate that if a global control of the solution is sought for, the incremental finite element analysis should be repeated from some earlier time instant by starting with a finer initial mesh [41].

6. NUMERICAL ILLUSTRATION

The aim of this example is to illustrate a methodology for the assessment of the quality of the finite element solution obtained with an incremental procedure and in presence of change of the finite element mesh at the time instant t_n. The methodology is presented on the one dimensional elastoplastic bar under distributed axial loads depicted in Figure 5.
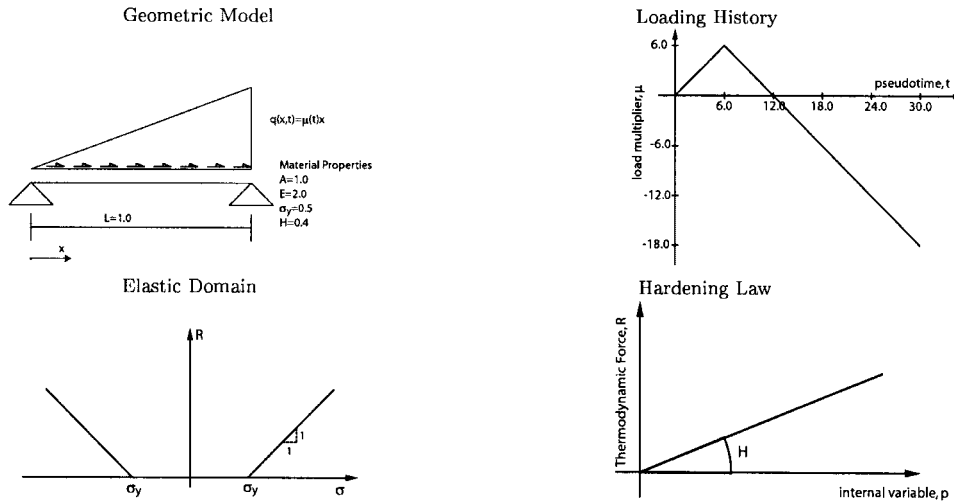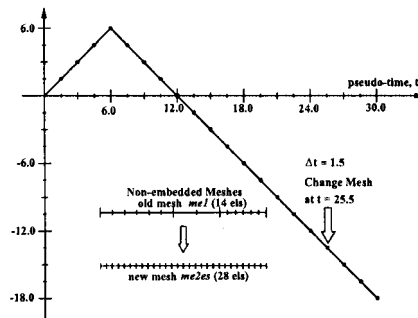
Figure 5. 1D Model problem.

Figure 6. Change between non-embedded meshes.

The bar is assumed to be composed of an elastoplastic material which obeys the Prandtl–Reuss plasticity law with linear hardening.

The initial discretization of the model problem is realized with uniform time step $\Delta t = 1.5$ and the non uniform mesh $me1$ of 14 linear elements depicted in Figure 6.

A prescribed type of change of mesh between non-embedded meshes is assumed to occur at the time $t_n = 25.5$. At this time instant plastic loading starts to localize once the load has been reversed in sign. The condition $\mathscr{V}^{h_n} \subset \mathscr{V}^{h_{n+1}}$ is not realized. Nevertheless, the mesh associated with $\mathscr{V}^{h_{n+1}}$ is chosen to contain a larger number of elements. In particular, the new mesh $me2es$ has been obtained by considering 28 linear equally spaced finite elements. Figure 6 shows the time discretization and the time instant when the change from the old mesh $me1$ to the new mesh $me2es$ occurs.

Three types of definition of initial state $\tilde{\varepsilon}_n^{\mathrm{p}}(x)$, $\tilde{p}_n(x)$ on the new mesh *me2es* to restart the finite element analysis at the time $t_n = 25.5$ have been taken into account. These definitions exemplify the three groups of transfer procedures introduced in Section 5.

The variationally consistent transfer is obtained by sampling at the Gauss points of the new mesh the fields $^{h_n}\varepsilon_n^{\mathrm{p}}(x)$ and $^{h_n}p_n(x)$, whose distribution assumption must comply with the requirements dictated by Equation (32). Here, these fields have been obtained over each element as prolongation into a constant function of the value at the respective unique Gauss point used for the quadrature of the elemental contribution to the internal virtual power.

The initial state $\tilde{\varepsilon}_n^{\mathrm{p}}(x)$, $\tilde{p}_n(x)$ obtained from the weak enforcement of the continuity with the fields $^{h_n}\varepsilon_n^{\mathrm{p}}(x)$, $^{h_n}p_n(x)$, which is hereafter referred to as the L^2 transfer, is given by

$$\forall e = 1, 2, \ldots, N_{h_{n+1}}$$

$$(\tilde{\bullet})_n^{\mathrm{e}}(x) = \frac{\displaystyle\int_{x_{\mathrm{e}}^{h_{n+1}}}^{x_{\mathrm{e}+1}^{h_{n+1}}} {}^{h_n}(\bullet)_n(x)\, \mathrm{d}x}{x_{\mathrm{e}+1}^{h_{n+1}} - x_{\mathrm{e}}^{h_n}} \quad \forall x \in]x_{\mathrm{e}}^{h_{n+1}}, x_{\mathrm{e}+1}^{h_{n+1}}[\tag{38}$$

where $N_{h_{n+1}}$ is the number of elements in the triangulation $\mathscr{T}_{h_{n+1}}$ and the superscript 'e' stands for element. The transfer defined by Equation (38) assumes a constant value for $(\tilde{\bullet})_n^{\mathrm{e}}(x)$ over each element $\Omega_{\mathrm{e}}^{h_{n+1}} \in \mathscr{T}_{h_{n+1}}$. This value is equal to the weighted average of the field $^{h_n}(\bullet)_n(x)$, with the weight given by the area of the so called tributary regions. For the problem at hand, these regions are defined as the parts of the element, $\Omega_{\mathrm{e}}^{h_{n+1}} = [x_{\mathrm{e}}^{h_{n+1}}, x_{\mathrm{e}+1}^{h_{n+1}}]$, of the new mesh where the field $^{h_n}(\bullet)_n(x)$ is constant.

Finally, the transfer introduced in Reference [21] has been used as an example of smoothing transfer. Once the data $\tilde{\varepsilon}_n^{\mathrm{p}}$, $\tilde{p}_n$ at the Gauss points of the new mesh have been assigned, we consider the finite element solution at t_n^+ corresponding to load increment equal to zero, i.e. load level equal to $q(x, t_n) = \mu(t_n)x$. This delivers a system state which is in equilibrium with respect to the new mesh.

Plastic strain $^{h_{n+1}}\varepsilon_n^{\mathrm{p}}$ and accumulated plastic strain $^{h_{n+1}}p_n$ obtained at the single Gauss points of each element of the new mesh are prolongated into a uniform field over the respective element. The effects of the data equilibration for each transfer are visualized in Figure 7. Here, a variation of the initial state defined by the given transfer procedure is noted. In particular, then, a saw-tooth distribution has been obtained in the case of L^2 transfer. In this same picture we have also plotted the distributions $^{h_n}\varepsilon_n^{\mathrm{p}}(x)$, $^{h_n}p_n(x)$ so that one can appreciate the discontinuity jump of these fields at t_n as a result of the change of mesh.

The corresponding admissible solutions necessary to compute the augmented extended dissipation error are obtained following the criteria given in Box 2. The distributions of the admissible plastic strain and the admissible accumulated plastic strain at t_n^- and t_n^+ are depicted in Figure 8 which shows the time discontinuity in these fields.

The accumulated plastic strain $p_{\mathrm{ad}}(x, t_n^+)$ differs from the corresponding finite element solution in almost all elements for all the transfers. This difference is due to the definition of $p_{\mathrm{ad}}(x, t_n^+)$ in terms of $\Delta\varepsilon_{\mathrm{ad}}^{\mathrm{p}}(x)$ and $p_{\mathrm{ad}}(x, t_n^-)$ and represents an essential feature in the assessment of the global quality in time of the solution. In fact, $p_{\mathrm{ad}}(x, t_n^-)$ accounts for the history of the solution up to the current time t_n whereas the finite element solution $^{h_{n+1}}p_n(x)$
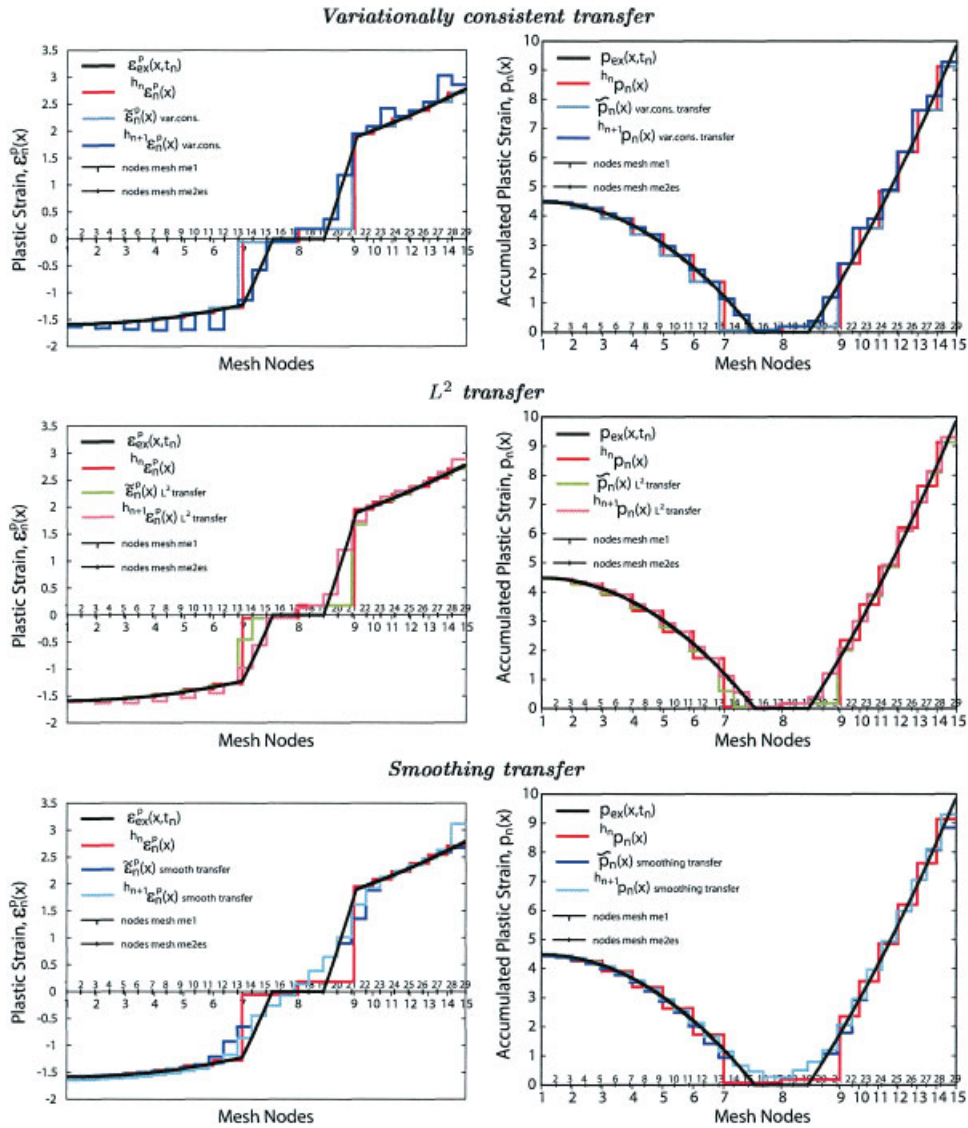
Figure 7. Plastic strain and accumulated plastic strain distribution at $t_n = 25.5$ resulting from different transfer operations.

is computed in terms of $\tilde{p}_n(x)$. The latter field is given by the specific transfer procedure, thus, information on the accuracy associated with the past values of the solution could be lost. The definition of p_{ad}, on contrary, accounts for the approximations associated with the variable up to the current time t_n.
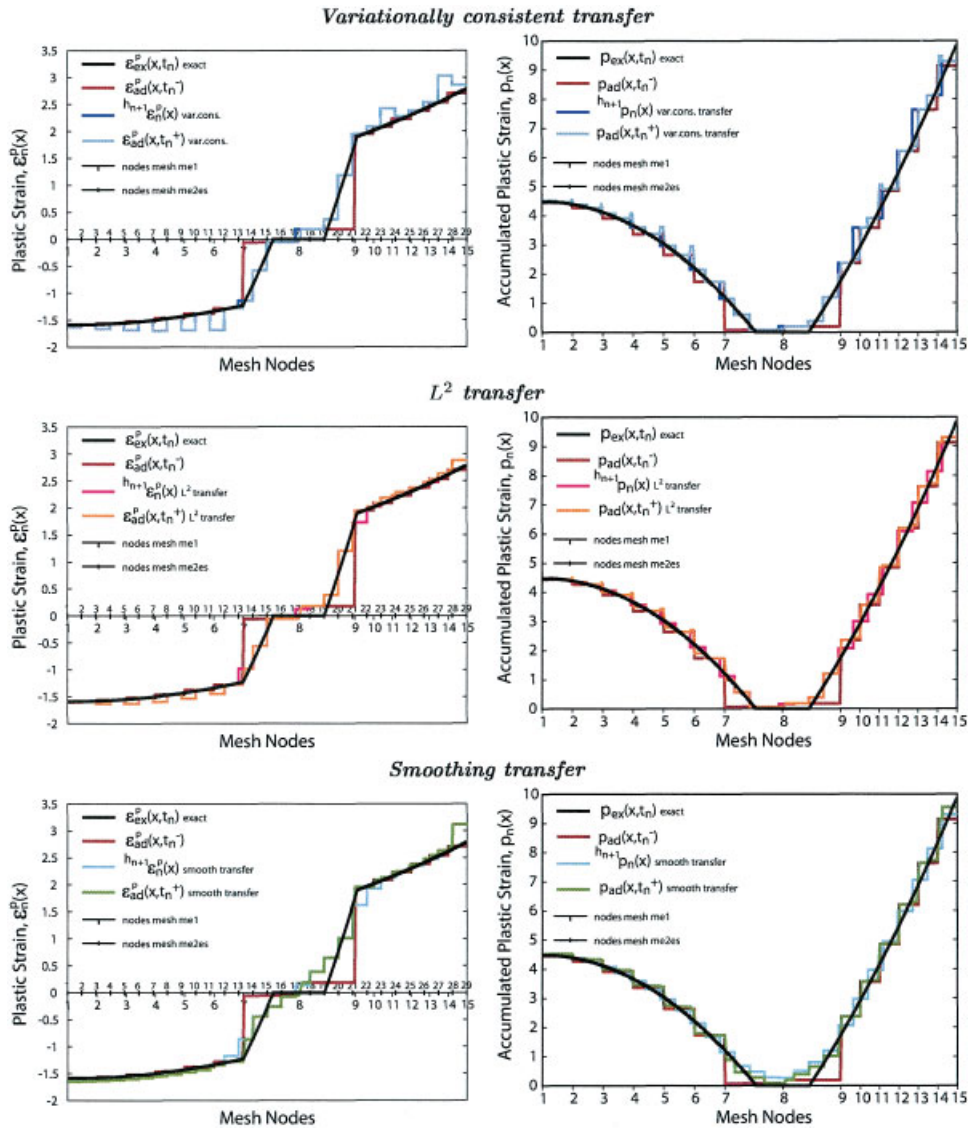
Int. J. Numer. Meth. Engng 2004; **60**:1595–1631

Figure 8. Admissible plastic strain and admissible accumulated plastic strain distribution at $t_n = 25.5^-$, $t_n = 25.5^+$ and plots of $^{h_{n+1}}(\bullet)_n(x)$ obtained from equilibration of the data with respect to the new mesh.

The time evolutions of the augmented extended dissipation error of the admissible solutions corresponding to the finite element solutions resulting from the three different transfers are given in Figure 9. All the diagrams present similar qualitative behaviour. A global improvement of the quality of the solution by considering the proposed transfers for the given change of mesh is noted. In particular, the solution resulting from L^2 transfer appears to behave slightly better
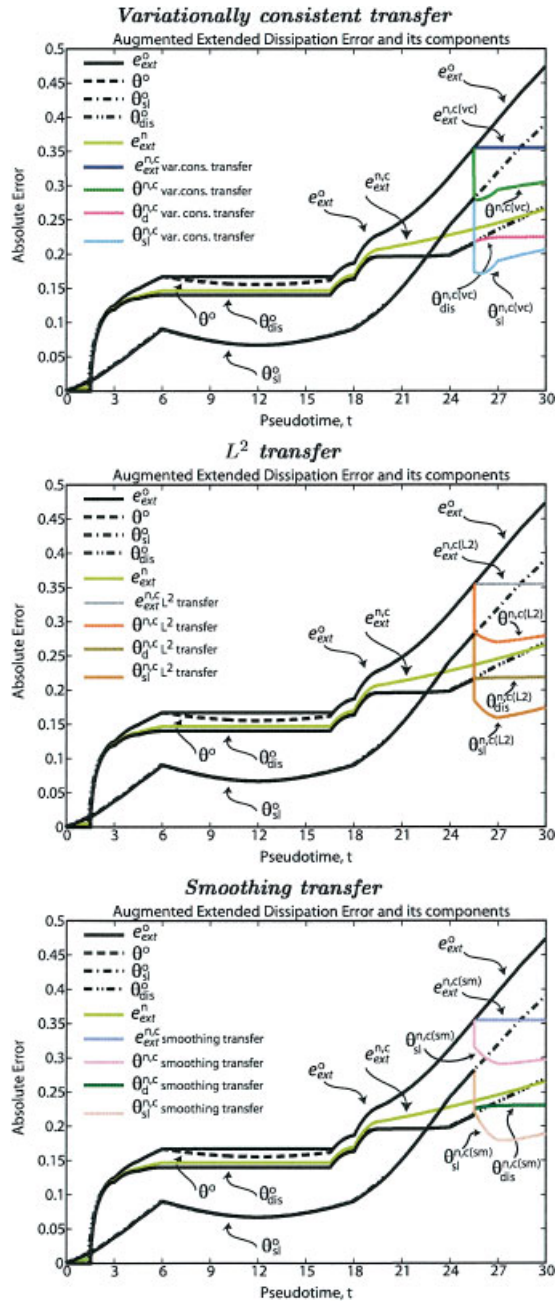
Figure 9. Time evolution of the augmented extended dissipation error with its components for different type of transfer at $t_n = 25.5$. Variationally consistent, L^2 and smoothing transfer.
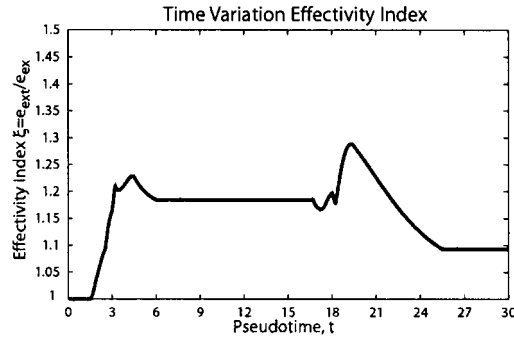
Figure 10. Evolution in time of the effectivity index.

out of the proposed transfer procedures. This is shown by the time variation of the current error $\theta^{n,c}(t)$. In the case of the L^2 transfer, the evolution of $\theta^{n,c}(t)$ is the closest to $e_{\mathrm{ext}}^n(t)$, where $e_{\mathrm{ext}}^n(t)$ is the extended dissipation error which is obtained with the dense finite element mesh *me2es* that is constant throughout the loading process.

The extended dissipation error computed at each time t_i, as given by Equation (36), and the error in solution, as given by Equation (29), have been used to define the effectivity index

$$\xi(t) = \frac{e_{\mathrm{ext}}(t)}{e_{\mathrm{ex}}(t)} \tag{39}$$

as is usually done for elliptic problems [42]. The time evolution of $\xi(t)$, shown in Figure 10 is identical for all the schemes resulting from the different transfer assumptions. Both the augmented extended dissipation error and the exact error which enter Equation (39) involve L^∞ control in time. Consequently, following the change of mesh, reduction of the error with value equal to the one related to the same initial mesh *me1* is obtained.

Tables I and II contain the values at t_n^-, t_n^+ and t_{n+1} of the several components of the augmented extended dissipation error defined by Equation (36). This table allows one to appreciate the differences between different transfer procedures and the corresponding importance of the additional term $^{\Delta}\theta_d$ on the current error θ. For completeness, we have also given the values which are obtained by assuming the finite element meshes *me1* and *me2es* constant in time during the whole loading process, whereas the values at the time t_{n+1} are reported to illustrate the influence of the transfer procedure at a later time.

When the variationally consistent transfer is used, the lowest value of the free energy norm of the error, $\theta_{\mathrm{sl}}^{n,c}$, at t_n^+ is attained. This is essentially the result of the best fit between the admissible stress and the stress conjugate to the admissible elastic strain as shown in Figure 11. The fit between the admissible thermodynamic forces and the forces conjugate to the admissible accumulated plastic strain, depicted in Figure 12, conversely, appears to be best in the case of the L^2 transfer. As for the effects of the transfer, with the adoption of the variationally consistent transfer, the non-uniform redistribution of the initial state $\tilde{\varepsilon}_n^{\mathrm{p}}$, $\tilde{p}_n$ following the equilibration of the data produces concentration of plastic strain in the elements 23 and 27. This, in turn, gives rise to an admissible accumulated plastic distribution $p_{\mathrm{ad}}(x, t_n^+)$ which is substantially different from the distribution of the admissible hardening forces at t_n^+. This difference is kept also at

Table I. Comparison of the error components at time $t_n = 25.5$ and $t_{n+1} = 27.0$.

| | $t_n = 25.5$ | | | | | | |
	e_{ext}	θ	θ_{sl}	$\dfrac{\theta_{\text{sl}}^{\text{e}}}{\theta_{\text{sl}}^{\text{p}}}$	θ_d	$\Delta\theta_d$	$\Delta\theta_d/\theta$
$me1$	0.355	0.355	0.282	$\dfrac{0.141}{0.244}$	0.215	—	—
$me2es$	0.236	0.236	0.131	$\dfrac{0.057}{0.118}$	0.196	—	—
$me1 \rightarrow me2es$ Var. transfer	0.355 t_n^+	0.278 t_n^+	0.173 t_n^+	$\dfrac{0.076}{0.156}$	0.218 t_n^+	0.033	0.12
$me1 \rightarrow me2es$ L^2 transfer	0.355 t_n^+	0.284 t_n^+	0.184 t_n^+	$\dfrac{0.110}{0.148}$	0.216 t_n^+	0.014	0.05
$me1 \rightarrow me2es$ Sm. transfer	0.355 t_n^+	0.316 t_n^+	0.222 t_n^+	$\dfrac{0.144}{0.168}$	0.225 t_n^+	0.064	0.20

Table II. Comparison of the error components at time $t_{n+1} = 27.0$.

| | $t_n = 27.0$ | | | | | |
	e_{ext}	θ	θ_{sl}	$\dfrac{\theta_{\text{sl}}^{\text{e}}}{\theta_{\text{sl}}^{\text{p}}}$	θ_d	$\Delta\theta_d/\theta$
$me1$	0.396	0.396	0.319	$\dfrac{0.160}{0.276}$	0.235	—
$me2es$	0.245	0.245	0.146	$\dfrac{0.063}{0.132}$	0.197	—
$me1 \rightarrow me2es$ Var. transfer	0.355	0.294	0.190	$\dfrac{0.075}{0.174}$	0.224	0.11
$me1 \rightarrow me2es$ L^2 transfer	0.355	0.270	0.159	$\dfrac{0.074}{0.141}$	0.218	0.05
$me1 \rightarrow me2es$ Sm. transfer	0.355	0.291	0.179	$\dfrac{0.081}{0.160}$	0.229	0.22

t_{n+1} and is the cause of the increase of the error associated with the residual in the hardening law at the time t_{n+1}.

With the L^2 and smoothing transfer, on contrary, the error in the state law at t_{n+1} decreases with respect to t_n^+. This decrease can be considered due mainly to the enhanced approximation properties of the new interpolation space whose effects are soon evident on the variation of admissible plastic strain. Therefore, for these two transfers, unlike the variationally consistent transfer, the values of the error at t_n^+ can be assumed to reflect the effects more pertinent to the transfer procedure. For the variationally consistent transfer, on contrary, also the value of the error at t_{n+1} must be considered.
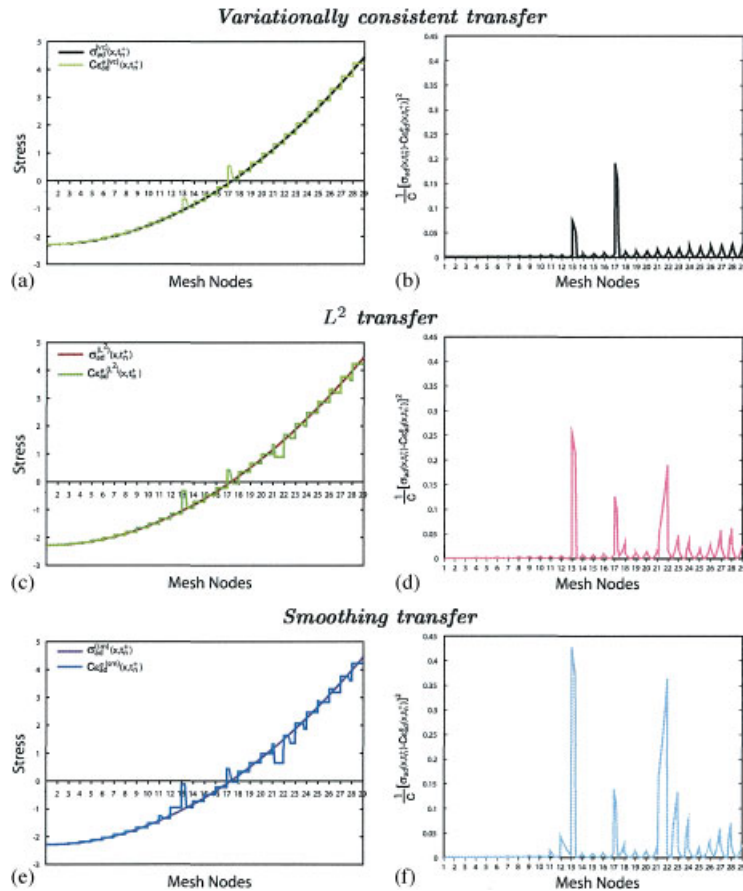
Figure 11. The error in the elastic law at $t = 25.5^+$ after change of mesh with different transfer operations: (a) variationally consistent transfer: admissible stress σ_{ad} versus stress conjugate of the admissible elastic strain $C\varepsilon^e_{ad}$; (b) variationally consistent transfer: pointwise contribution to the error in the elastic law, $\frac{1}{C}(\sigma_{ad} - C\varepsilon^e_{ad})^2$; (c) L^2 transfer: admissible stress σ_{ad} versus stress conjugate of the admissible elastic strain $C\varepsilon^e_{ad}$; (d) L^2 transfer: pointwise contribution to the error in the elastic law, $\frac{1}{C}(\sigma_{ad} - C\varepsilon^e_{ad})^2$; (e) smoothing transfer: admissible stress σ_{ad} versus stress conjugate of the admissible elastic strain $C\varepsilon^e_{ad}$; and (f) smoothing transfer: pointwise contribution to the error in the elastic law, $\frac{1}{C}(\sigma_{ad} - C\varepsilon^e_{ad})^2$.

Finally, for the model under consideration and further to the definition of the admissible solutions, it follows [32]

$$\Delta_{\zeta^2_d}(x, t_n) = \frac{\|\Delta\varepsilon^p_{ad}\|}{2}\left[R_0 + R_{ad}(x, t_n^+) - \|\sigma^D_{ad}(x, t_n^+)\|\right] + \frac{\|\Delta\varepsilon^p_{ad}\|}{2}\left[R_0 + R_{ad}(x, t_n^-) - \|\sigma^D_{ad}(x, t_n^-)\|\right]$$

(40)

where, in general, $f(\sigma_{ad}, R_{ad}) = R_0 + R_{ad}(x, t) - \|\sigma^D_{ad}(x, t)\| \geqslant 0$.
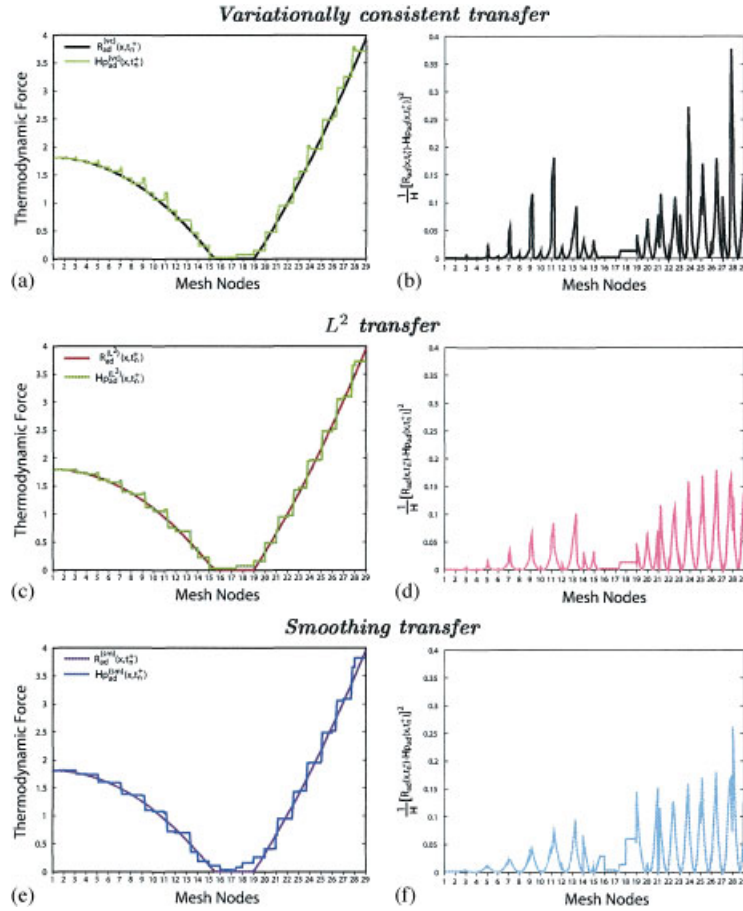
Figure 12. The error in the hardening law at $t = 25.5^+$ after change of mesh with different transfer operations: (a) variationally consistent transfer: admissible thermodynamic force R_{ad} versus force conjugate of the admissible accumulated plastic strain Hp_{ad}; (b) variationally consistent transfer: pointwise contribution to the error in the hardening law, $\frac{1}{H}(R_{ad} - Hp_{ad})^2$; (c) L^2 transfer: admissible thermodynamic force R_{ad} versus force conjugate of the admissible accumulated plastic strain Hp_{ad}; (d) L^2 transfer: pointwise contribution to the error in the hardening law, $\frac{1}{H}(R_{ad} - Hp_{ad})^2$; (e) smoothing transfer: admissible thermodynamic force R_{ad} versus force conjugate of the admissible accumulated plastic strain Hp_{ad}; and (f) smoothing transfer: pointwise contribution to the error in the hardening law, $\frac{1}{H}(R_{ad} - Hp_{ad})^2$.

Thus, Figures 13–15 allow comparisons of the different contributions to the jump term $^{\Delta}\theta_d(t_n) = \int_{\Omega} {}^{\Delta}\zeta_d^2(x, t_n)\, dx$ for the transfer procedures under consideration. These are obtained by comparing the plastic strain, which is introduced by the transfer, to the evolution of the admissible generalized stress field. In particular, the contribution appears to be highest in the case of the smoothing transfer assumption as a result of the so-called diffusion of plastic strain. The smoothing transfer assumption produces in the elements 15,16 and 18 a variation
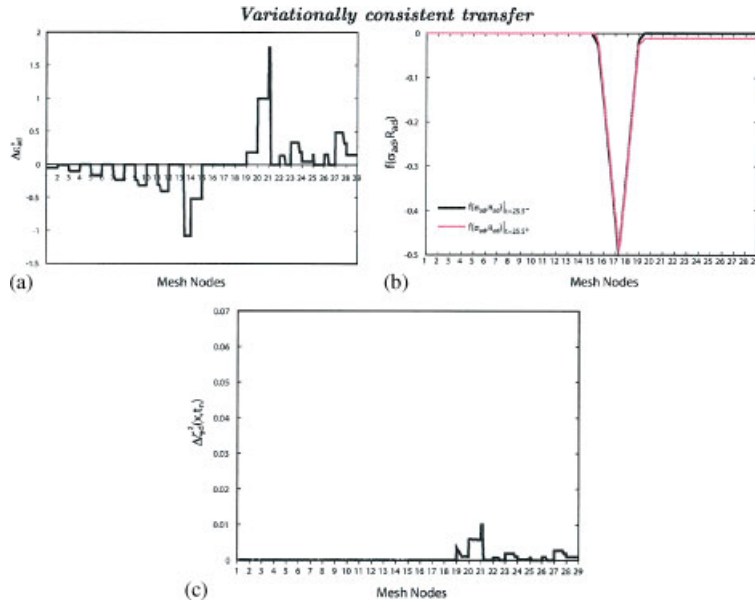
Figure 13. Variationally consistent transfer: (a) variation of admissible plastic strain at $t_n = 25.5$; (b) space distribution of $f(\sigma_{ad}, R_{ad})$ at t_n^- and t_n^+; and (c) pointwise contribution to the jump term $^\Delta\theta_d(t_n)$.
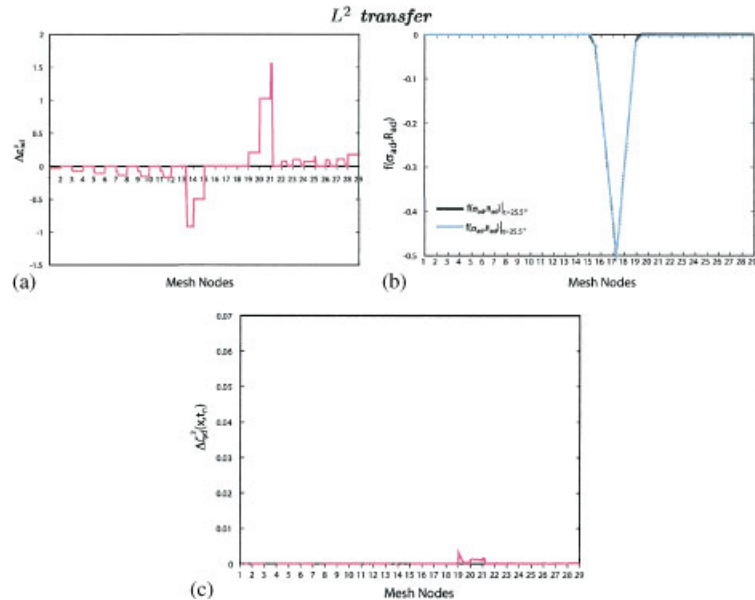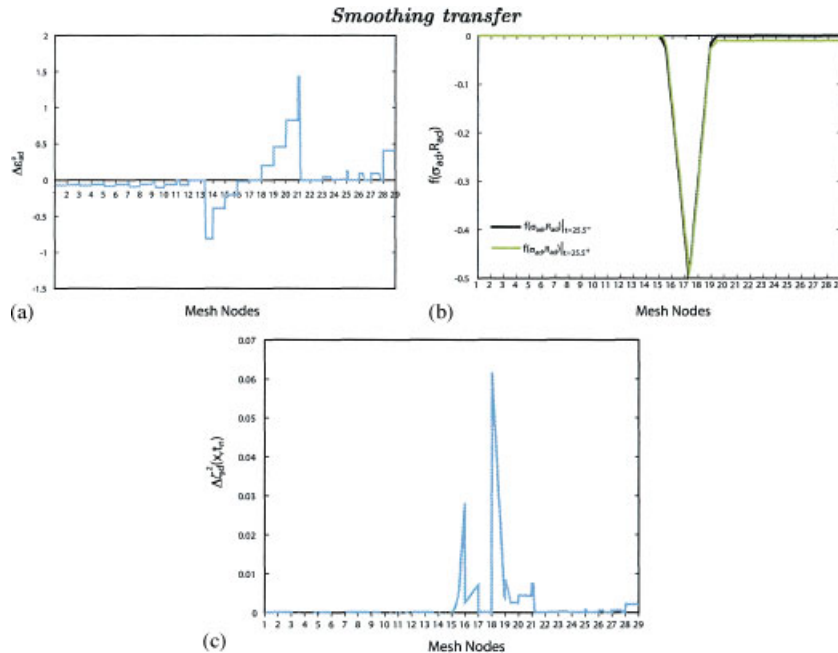

Figure 14. L^2 transfer: (a) variation of admissible plastic strain at $t_n = 25.5$; (b) space distribution of $f(\sigma_{ad}, R_{ad})$ at t_n^- and t_n^+; and (c) pointwise contribution to the jump term $^\Delta\theta_d(t_n)$.

Figure 15. Smoothing transfer: (a) variation of admissible plastic strain at $t_n = 25.5$; (b) space distribution of $f(\sigma_{\text{ad}}, R_{\text{ad}})$ at t_n^- and t_n^+; and (c) pointwise contribution to the jump term $^\Delta\theta_d(t_n)$.

of admissible plastic strain, as shown in Figure 15(a), whereas the variation of $f(\sigma_{\text{ad}}, R_{\text{ad}})$, given in Figure 15(b) indicates that the behaviour associated with $(\sigma_{\text{ad}}, R_{\text{ad}})$ should be elastic, since $f \leqslant 0$ therein.

7. CONCLUSIONS

In this work, we have presented a general methodology for the assessment of the global quality of displacement finite element solutions of elastoplastic problems discretized in time with the backward Euler method on dynamically changing mesh. With this regard, a new measure of the error in the constitutive equations which account for time discontinuity jumps in the admissible solution has been developed.

With the methodology set in this work, a more rational treatment of the transfer operation seems possible to be devised in the context of the ensuing error. This should therefore lead to the definition of a transfer operation such as the one that minimizes the error produced. The definition of time step size, mesh size and indication on how to change mesh and to give data are not separate steps arising from heuristic arguments but should result from a unified analysis of the error contribution of each component.

One aspect of the future research effort will focus on implementation and numerical assessment of the described procedure for higher dimensional problems.

REFERENCES

1. Zienkiewicz OC, Zhu JZ. A simple error estimator and adaptive procedure for practical engineering analysis. *International Journal for Numerical Methods in Engineering* 1987; **24**:337–357.
2. Zienkiewicz OC, Liu YC, Huang GC. Error estimation and adaptivity in flow formulation for forming problems. *International Journal for Numerical Methods in Engineering* 1988; **25**:23–42.
3. Ortiz M, Quigley JJ. Adaptive mesh refinement in strain localization problems. *Computer Methods in Applied Mechanics and Engineering* 1991; **90**:781–804.
4. Perić D, Yu J, Owen DRJ. On error estimates and adaptivity in elastoplastic solids: applications to the numerical simulation of strain localization in classical and Cosserat continua. *International Journal for Numerical Methods in Engineering* 1994; **37**:1351–1379.
5. Johnson C, Hansbo P. Adaptive finite element methods in computational mechanics. *Computer Methods in Applied Mechanics and Engineering* 1992; **101**:143–181.
6. Repin SI, Xanthis L. A posteriori error estimation for elasto-plastic problems based on duality theory. *Computer Methods in Applied Mechanics and Engineering* 1996; **138**:317–339.
7. Rannacher R, Suttmeier FT. A posteriori error control in finite element methods via duality techniques: application to perfect plasticity. *Computational Mechanics* 1998; **21**:123–133.
8. Alberty J, Carstensen C. Numerical analysis of time-depending primal elastoplasticity with hardening. *SIAM Journal on Numerical Analysis* 2000; **37**:1271–1294.
9. Rannacher R, Suttmeier FT. A posteriori error estimation and mesh adaptation for finite element models in elasto-plasticity. *Computer Methods in Applied Mechanics and Engineering* 1999; **176**:333–361.
10. Barthold FJ, Schmidt M, Stein E. Error indicators and mesh refinements for finite-element-computations of elastoplastic deformations. *Computational Mechanics* 1998; **22**:225–238.
11. Ladevèze P. Comparaison de modèles de milieux continus. *Ph.D. Thesis*, Université Pierre et Marie Curie-Paris 6, France, 1975.
12. Ladevèze P. Sur une famille d'algorithmes en mécanique des structures. *Comptes Rendus Académie des Sciences, II* 1985; **300**:41–44.
13. Ladevèze P. La méthode à grand incrément de temps pour l'analyse des structures à comportement non linéaire décrit par variables internes. *Comptes Rendus Académie des Sciences, II* 1989; **309**:1095–1099.
14. Ladevèze P. Moës N, Douchin B. Constitutive relation error estimators for (visco)plastic finite element analysis with softening. *Computer Methods in Applied Mechanics and Engineering* 1999; **176**:247–264.
15. Orlando A, Perić D. A study on a posteriori error estimation for elastoplastic solids. In *Proceedings of the 6th International Conference on Computational Plasticity—COMPLAS VI*, Barcelona, 2000.
16. Cirak F, Ramm E. A posteriori error estimation and adaptivity for elastoplasticity using the reciprocal theorem. *International Journal for Numerical Methods in Engineering* 2000; **47**:379–393.
17. Eriksson K, Johnson C. Adaptive finite element methods for parabolic problems I: a linear model problem. *SIAM Journal on Numerical Analysis* 1991; **28**:43–77.
18. Eriksson K, Estep D, Hansbo P, Johnson C. *Computational Differential Equation*. Cambridge University Press: Cambridge, 1996.
19. Chen Z, Nochetto RH, Schmidt A. Error control and adaptivity for a phase relaxation model. *ESAIM-Mathematical Modelling and Numerical Analysis-Modelisation Mathematique et Analyse Numerique* 2000; **34**:775–797.
20. Wiberg NE, Li XD. Adaptive finite element procedures for linear and non-linear dynamics. *International Journal for Numerical Methods in Engineering* 1999; **46**:1781–1802.
21. Perić D, Hochard Ch, Dutko M, Owen DRJ. Transfer operators for evolving meshes in small strain elasto-plasticity. *Computer Methods in Applied Mechanics and Engineering* 1996; **137**:331–344.
22. Rashid MM. Material state remapping in computational solid mechanics. *International Journal for Numerical Methods in Engineering* 2002; **55**:431–450.
23. Ladevèze P. *Nonlinear Computational Structural Mechanics*. Springer: Berlin, 1999.

24. Halphen B, Nguyen QS. Sur les materiaux standards generalises. *Journal de Mécanique* 1975; **14**:39–63.
25. Rockafellar RT. *Convex Analysis*. Princeton University Press: Princeton, 1970.
26. Ekeland I, Temam R. *Convex Analysis and Variational Problems*. North-Holland: Amsterdam, 1976.
27. Lemaitre J, Chaboche JL. *Mechanics of Solid Materials*. Cambridge University Press: Cambridge, 1990.
28. Coleman BD, Gurtin ME. Thermodynamics with internal state variables. *The Journal of Chemical Physics* 1967; **47**:597–613.
29. Germain P, Nguyen QS, Suquet P. Continuum thermodynamics. *Journal of Applied Mechanics—Transactions of the ASME* 1983; **50**:1010–1020.
30. Ladevèze P, Pelle JP. *La Maitrise du Calcul en Mécanique Linéaire et Non Linéaire*, Hermes Science Publications: Paris, 2001.
31. Bataille J, Kestin J. Irreversible processes and physical interpretation of rational thermodynamics. *Journal of Non-equilibrium Thermodynamics* 1979; **4**:229–258.
32. Orlando A. Analysis of adaptive finite element solutions in elastoplasticity with reference to transfer operation techniques. *Ph.D. Thesis* C/Ph/258/02, University of Wales, Swansea, UK, in preparation.
33. Mikusinski J, Sikorski R. *The Elementary Theory of Distributions*. Panstwowe Wydawnictwo Naukowe: Warsawa, 1957.
34. Zienkiewicz OC, Taylor RL. *The Finite Element Method* (5th edn), vol. 1–3. Butterworth-Heinemann: Stoneham, MA, 2000.
35. Camacho GT, Ortiz M. Adaptive Lagrangian modelling of ballistic penetration of metallic targets. *Computer Methods in Applied Mechanics and Engineering* 1997; **142**:269–301.
36. Radovitzky R, Ortiz M. Error estimation and adaptive meshing in strongly nonlinear dynamic problems. *Computer Methods in Applied Mechanics and Engineering* 1999; **172**:203–240.
37. Fraeijs de Veubeke B. Displacement and equilibrium models in the finite element method. In *Stress Analysis*, Zienkiewicz OC, Holister GS (eds), Chapter 9. Wiley: New York, 1965; 145–197.
38. Lee N, Bathe KJ. Error indicators and adaptive remeshing in large deformation finite element analysis. *Finite Elements in Analysis and Design* 1994; **16**:99–139.
39. Ladevèze P, Moës N. A new a posteriori error estimation for nonlinear time dependent finite element analysis. *Computer Methods in Applied Mechanics and Engineering* 1997; **157**:45–68.
40. Ladevèze P, Leguillon D. Error estimate procedure in the finite element method and applications. *SIAM Journal on Numerical Analysis* 1983; **20**:485–509.
41. Ladéveze P, Coffignal G, Pelle JP. Accuracy of elastoplastic and dynamic analysis. In *Accuracy Estimates and Adaptive Refinements in Finite Element Computations*, Babuska I, Zienkiewicz OC, Gago J, de A. Oliveira ER (eds), Chapter 11. Wiley: New York, 1986; 181–203.
42. Babuska I, Rheinboldt WC. A posteriori error estimates for the finite element method. *International Journal for Numerical Methods in Engineering* 1978; **12**:1597–1615.
43. Coffignal G. Optimisation et Fiabilité des Calculs Eléments Finis en Elastoplasticité. *Ph.D. Thesis*, Université Pierre et Marie Curie-Paris 6, France, 1987.